LAWRENCE
LIVERMORE
NATIONAL
LABORATORY

LLNL-TR-458596

Environmental Transport of Plutonium: Biogeochemical Processes at Femtomolar Concentrations and Nanometer Scales

A. B. Kersting

October 6, 2010

Disclaimer

This work performed under the auspices of the U.S. Department of Energy by Lawrence Livermore National Laboratory under Contract DE-AC52-07NA27344.

FY10 LLNL SFA Program Management and Performance Report:

Environmental Transport of Plutonium: Biogeochemical Processes at Femtomolar Concentrations and Nanometer Scales

Laboratory Research Manager:
Annie Kersting
Director, Glenn T. Seaborg Institute
Physical & Life Sciences Directorate
Lawrence Livermore National Laboratory
L-231, Livermore CA 94550
925 432-2228
Kersting1@LLNL.gov

Laboratory Lead Scientist:
Mavrik Zavarin

Collaborators:
Brian Powell[2], Duane Moser[3], Susan Carroll[1], Robert Maxwell[1], Zurong Dai[1], Ross Williams[1], Scott Tumey[1], Pihong Zhao[1], Ruth Tinnacher[1], Patrick Huang[1], Ruth Kips[1], Harris Mason[1], James Begg[1], Jen Fisher[3], Laura Simpkin[2], Trevor Zimmerman[2], Joseph Jablonski[2] Matthew Snow[1].

[1]Lawrence Livermore National Laboratory, [2]Clemson University, [3]Desert Research Institute

TABLE of CONTENTS

1. Program Overview

The major challenge in predicting the mobility and transport of plutonium (Pu) is determining the dominant geochemical processes that control its behavior in the subsurface. The reaction chemistry of Pu (*i.e.*, aqueous speciation, solubility, sorptivity, redox chemistry, and affinity for colloidal particles, both abiotic and microbially mediated) is particularly complicated. It is generally thought that due to its low solubility and high sorptivity, Pu migration in the environment occurs only when facilitated by transport on particulate matter (*i.e.*, colloidal particles). Despite the recognized importance of colloid-facilitated transport of Pu, very little is known about the geochemical and biochemical mechanisms controlling Pu-colloid formation and association, particularly at femtomolar Pu concentrations observed at DOE sites.

Reactive transport models that address geochemical processes occurring at the mineral-water interface are still in their infancy for multi-phase systems (U.S. DEPARTMENT OF ENERGY, 2007). Generally, existing transport models have ignored the coupled factors of redox chemistry and microbial activity and have relied on empirical equilibrium or rate-limited distribution coefficient (K_d) models to address actinide retardation and colloid-facilitated transport (*e.g.*, (GLYNN, 2003; PICKETT, 2005; TIEN and JEN, 2007). Recent experimental data from Powell and others (KAPLAN et al., 2004; POWELL et al., 2005; KAPLAN et al., 2006; DEMIRKANLI et al., 2008;) suggest that these simplified models cannot adequately predict Pu transport because they do not capture the coupled processes controlling Pu sorption and desorption.

This 5-year program is designed to test the important biogeochemical processes governing colloid-facilitated Pu transport in the field. We hypothesize that biogeochemical processes operating under low (10^{-9} – 10^{-16} mol/L), environmentally relevant, concentrations are fundamentally different from those operating in simple, binary-system laboratory experiments conducted at high Pu concentrations (10^{-4} – 10^{-9} mol/L). At environmentally relevant concentrations, Pu will be controlled by one or more of the following processes:

- binary sorption to low-site-density, high-affinity colloid surface sites (*e.g.*, surface defects),
- stabilization of Pu surface complexes on mineral colloids by natural organic matter coatings,
- surface precipitation of Pu polymers: experimental and natural nano-colloids,
- co-precipitation with colloids as a result of mineral alteration, and
- direct and indirect microbial interactions with Pu and colloids.

Our hypothesis is being tested by selectively examining each process separately as a function of concentration and then evaluating its potential role in Pu transport. Laboratory results are being compared to field samples taken from contaminated sites (NTS, RFETS, the Hanford Reservation and Tomsk, Russia) where Pu-containing colloids/particles will be and characterized. The processes listed above form the basis for 5 Program Elements, each with its own hypothesis-driven research program. However, each Program Element includes tasks that integrate aspects of this research plan to address our central hypothesis. Program Elements include computational chemistry studies, controlled laboratory experiments, geochemical modeling, and field sample characterization efforts that address length scales from the atomic to the field scale.

2. Scientific Objectives

The objective of this science program is the identification and quantification of the biogeochemical processes that control the fate and transport of Pu at picomolar to attomolar (10^{-12} – 10^{-18} mol/L) concentrations. We are investigating the roles of mineral surface defects, ternary complexes, polymerization, co-precipitation/surface alteration, as well as direct and indirect microbial interactions on the affinity and sorption/desorption rates of Pu. With the use of unique state-of-the-art facilities at LLNL such as the accelerator mass spectrometer (AMS), a NuPlasma HR IsoProbe mass spectrometer (MC-ICPMS), the Transmission Electron Microscope (TEM), and the nano-secondary ion mass spectrometer (NanoSIMS), we are conducting laboratory experiments on colloids at environmentally relevant concentrations. A primary goal of this program is to provide the DOE with the scientific basis to support decisions for the remediation and long-term stewardship of legacy sites.

3. Program Structure

Dr. Kersting is the program manager and point of contact for this program. She is also Director of the LLNL branch of the Glenn T. Seaborg Institute (Seaborg Institute) and reports directly to the Associate Director of the Physical & Life Sciences (PLS) Directorate, Bill Goldstein. Henry Shaw is the point-of-contact for LLNL's, BER Programs and is the Acting Chief Scientist for PLS reporting directly to Bill Goldstein. This SFA program is managed through the Seaborg Institute and is aligned with the Seaborg Institute's research focus on environmental radiochemistry, nuclear forensics and super heavy element discovery.

Dr. Kersting communicates BER program needs to both the Lead Scientist, Dr. Zavarin, and Program Element leads, coordinates program execution, insures financial responsibility in spending, planning, and program direction. Monthly program meetings/teleconferences with all staff members leads will serve to communicate progress and ensure that the program goals are being met. Each Program Element has a lead scientist that reports to both the SFA manager (Dr. Kersting) and lead scientist (Dr. Zavarin). Dr. Kersting reports to both LLNL senior management and BER. Dr. Zavarin ensures that Program Element efforts at LLNL and collaborating institutions are aligned with the research outlined.

The majority of the experimental work (Program Elements A, C, and D) is led by LLNL scientists under the supervision of Dr. Zavarin in his environmental radiochemistry laboratories. Program Element B and E leads and their post-docs/graduate students have access to LLNL through the Laboratory's Visiting Scientist Program. The sorption/desorption experiments in Program Element B (B. Powell lead) is a coordinated effort between Clemson University and LLNL. The microbial work in Program Element E (D. Moser lead) is carried out at the Desert Research Institute in conjunction with the University of Nevada, Las Vegas radiochemistry facilities of K. Czerwinski. Characterization and isolation of microbial populations in Pu-contaminated groundwater at the NTS are coordinated through external programs (*e.g.*, UGTA). Groundwater and sediment sample collection at other field sites is being coordinated through targeted collaborations (Hanford (A. Felmy); Tomsk, Russia (S. Kalmykov).

In addition to the roles of Dr. Kersting and Dr. Zavarin discussed above, each team member is indentified below and their expertise briefly summarized.

Annie Kersting—Director of the Glenn T. Seaborg Institute at LLNL, which conducts research on environmental radiochemistry and nuclear forensics. She also oversees both the postdoc (~90 postdocs) and a summer student programs (~10- summer students) in the Nuclear Forensics. Her research focuses on actinide transport in the subsurface. Dr. Kersting is the program manager for this SFA and is the lead on Program Element C: Surface precipitation of Pu polymers and field samples. The focus is on characterization of colloids in experimental and field samples using the Titan S/TEM and NanoSIMS. She co-supervises postdocs Ruth Tinnacher, Ruth Kips and James Begg (FY10 new hire), and coordinates summer students.

Mavrik Zavarin—LLNL Project manager for the Underground Test Area (UGTA) program. The UGTA program is responsible for identifying the extent of radiologic contamination at the NTS. Dr. Zavarin has been involved in experimental and modeling studies of radionuclide chemistry at the mineral-water interface, mineral dissolution/precipitation kinetics, colloid-facilitated transport, and radionuclide reactive transport modeling. Dr. Zavarin is the Lead Scientists and is responsible for designing and overseeing Program Elements A-E. He is also the lead for Program Element A: Binary sorption to low-density high affinity surface sites. Dr. Zavarin will coordinate NTS field operations with UGTA sampling program for program Element E: microbial interactions. He co-supervises postdocs Ruth Tinnacher, and James Begg (FY10 new hire).

Brian Powell—Assistant professor, Clemson University, radiochemist. Prof. Powell's research focuses on understanding and quantifying the rates and mechanisms of actinide interactions with natural soils and synthetic minerals. He continues to be involved with experimental and modeling studies of long-term (12 to 25 year) Pu vadose zone transport at the Savannah River Site. Prof. Powell will coordinate activities between Clemson and LLNL and supervise a graduate student that will be carrying out graduate thesis work on this project at LLNL.

Duane Moser—Microbial Ecologist at the Desert Research Institute. Dr. Moser has over 15 years of experience in monitoring microorganisms and their activities in the environment with an emphasis on the deep subsurface, aquatic systems and bioremediation. Moser is experienced in molecular- and cultivation-based approaches for microbial detection and provides a full complement of microbiological tools and analyses for the team, both field and laboratory. He supervises postdoc Jen Fisher.

Pihong Zhao – Dr. Zhao is a radiochemist with over 16 years experience in environmental radiochemistry, waste form, thermodynamic data measurements for actinides and development of actinides separations using new extraction resins. Dr. Zhao serves as lab manager for the program and has daily oversight responsibility over post-doc and student laboratory activities as part of this SFA.
Robert Maxwell—Chemist with expertise application of nuclear magnetic resonance methods to the study of the structure and dynamics of materials. Polymer aging and degradation. Dissolution kinetics of silica polymorphs. Organic-inorganic composite materials.
Susan Carroll—Geochemist Dr. Carroll has conducted and published research for a variety of rock-water systems focusing on experimental surface chemistry, mineral kinetics, mobility of metal and radioactive contaminants, and geologic CO_2 sequestration. She supervises postdoc Harris Mason.
Zurong Dai—Physicist, materials scientist at LLNL. Dr. Dai has more than 20 years experience in structural characterization of natural and man-made materials by using TEM. His research focuses on crystal growth and crystallography, nano-materials synthesis and characterization, experimental measurement of electronic structure and optical properties of materials. Dr. Dai will be responsible for the TEM analyses.
Ross Williams—Isotope geochemist at LLNL, Dr. Williams is the laboratory manager for the Chemical Science Division's ICP-MS Facility and chief scientists for the multi-collector NuPlasma HR IsoProbe ICPMS. Dr. Williams sets the standard for isotope ratio mass spectrometry in the DOE complex. He has more than 20 years of experience in actinide radiochemistry and metrology. Dr. Williams will be responsible for measurement and interpretation of ICP-MS measurements.
Scott Tumey—Radioanalytical chemist at the LLNL Center for Accelerator Mass Spectrometry (CAMS). Dr. Tumey is a key member of the heavy-isotope group at CAMS and has played a central roe in developing AMS measurement capabilities for actinides. Dr. Tumey will oversee the preparation and measurement of samples by AMS, and helps design laboratory experiments so that they adequately reflect the sample requirements of AMS.
Ruth Tinnacher—Postdoctoral fellow at LLNL. Dr. Tinnacher's research focuses on parameters and processes that control the sorption, remobilization and transport behavior of actinides in the environment such as organic and inorganic colloids and metal sorption/desorption kinetics. She has several years of experience in conducting lab-scale experiments with uranium, Pu and various organic matter fractions using batch, static column and advective column systems. Dr. Tinnacher will conduct sorption/desorption experiments.
Ruth Kips—Postdoctoral fellow at LLNL. Dr. Kips' research focuses on nuclear safeguards and the application of micro-analytical tools to the analysis of sub-micrometer-sized actinide particles to determine their morphological, isotopic, and compositional characteristics using electron microscopy, X-ray diffraction, ICP-MS, and NanoSIMS. She will use the NanoSIMS to characterize field and experimentally derived colloids.
Harris Mason—Postdoctoral fellow at LLNL. Dr. Mason's research focuses on applying NMR spectroscopic techniques to investigate metal sorption reactions at the mineral/water interface. He will use these methods to investigate how Pu behaves at the silica interface.
Jen Fisher— Postdoctoral associate at the Desert Research Institute. Dr. Fisher's research focuses on the microbial ecology of extreme environments and the interaction of microorganisms with toxic metal(loid)s. She will be isolating and characterizing metal-reducing and exopolysaccharide-producing bacteria from the Nevada Test Site and using these organisms in sorption experiments with Pu.

4. Performance Milestones and Metrics

Table 4.1 shows the task plan schedule for five years for each of the five Program Elements. Each Program Elements is sub-divided into Tasks. However, all activities are closely integrated and as such timing of specific experiments, especially as proposed in out years, may be modified. Blue demarcations show the original planned schedule and the green shows where we have deviated for the original plan. The accomplishments and metrics for each Program Element will be summarized below.

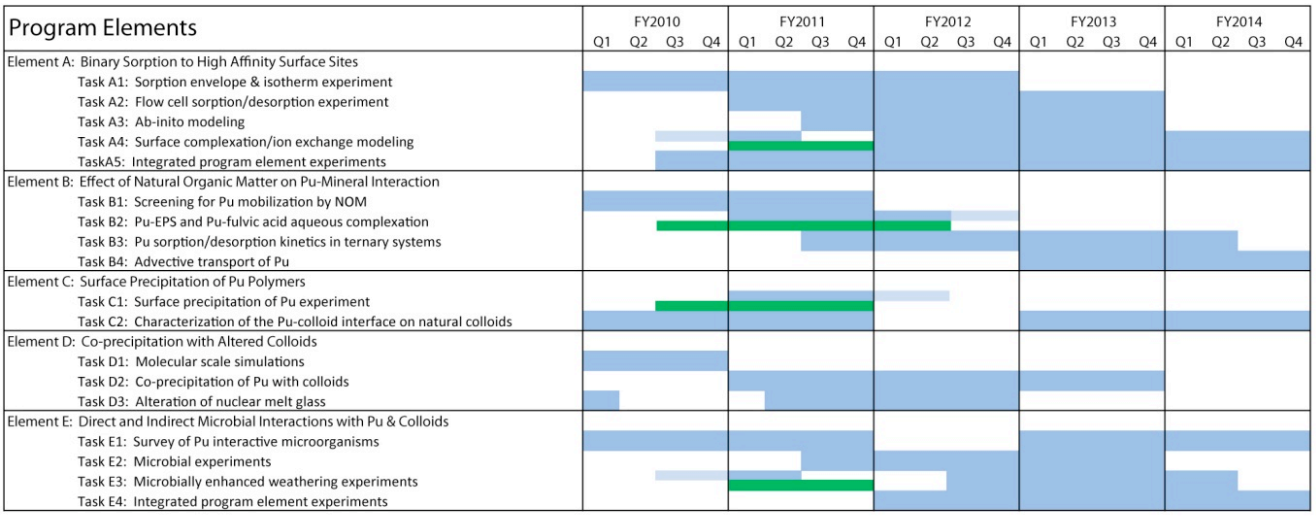

Table 4.1 Five year task plan subdivided into five Program Elements. The blue is the original plan, the green denotes where some projects were started earlier than originally planned. The lightest blue shows where projects were delayed.

4.a Review of Scientific Progress

4.a.i Brief Review of Scientific Progress

Program Element A: Binary Sorption to High-Affinity Surface Sites

(M. Zavarin: lead; P. Zhao, S. Tumey)

The focus of Program Element A is the study of Pu sorption in simple binary systems at Pu concentrations ranging from those observed in the field (attomolar to picomolar) to those commonly used in the lab (nanomolar to micromolar). The hypothesis guiding the effort in Program A is the following:

> *Colloid-facilitated Pu transport is fundamentally controlled by binary surface-complexation phenomena occurring on sites that have a range of sorption affinities, site-specific sorption/desorption kinetics, and redox transformation rates*

Testing this hypothesis requires collection of sorption data over a range of (1) solution conditions, (2) Pu concentrations, and (3) colloid minerals. The kinetics of sorption and desorption will be quantified and an understanding of the underlying mechanisms controlling sorption affinities and sorption/desorption kinetics identified. Based on the collected data, a surface complexation model that includes kinetics and hysteresis effects (if necessary) will be developed.

In FY10 the focus was to carry out a series of Pu sorption experiments on the common mineral, goethite (a-FeOOH). The first objective (Task A1) was to quantify the sorption behavior of both Pu(IV) and Pu(V) over a 10-order -of -magnitude concentration range. In addition we designed these experiments (Task A2) to test the lower limits of the accelerator mass spectrometry (AMS), NanoSIMS and TEM. We met both these milestones. Samples prepared at the higher concentrations were used as part of Program Element C, to begin to determine the boundaries for monomeric versus colloidal Pu formation. Task A3, *Ab initio* modeling was started this year instead of FY11 and was folded into Program Element D, Task D1: molecular scale simulations. Results are reported in Program Element D.

Task A1: Quantifying Pu Sorption Behavior on Geothite Over Ten Orders of Magnitude in Concentration Range

To investigate the effects of concentration on Pu sorption, we performed Pu(IV) and Pu(V) batch sorption isotherms in 0.7 mM $NaHCO_3$/5 mM NaCl (pH ~8) solution with goethite over a ten order of magnitude concentration range. While Pu(V) is known to reduce to Pu(IV) on the goethite surface (POWELL et al., 2005),

Pu(IV) and Pu(V) sorption was compared to determine whether a common equilibrium could be achieved regardless of the starting Pu oxidation state. Solution conditions were chosen such that aqueous Pu concentrations would range from 10^{-7} to 10^{-17} M while surface loading would range from >100% to $<10^{-7}$% (Figure A1). To quantify the aqueous Pu concentrations over this range, two Pu isotope compositions and several quantification techniques were employed (AMS, NuPlasma HR IsoProbe mass spectrometry, quadrupole ICP-MS, and traditional scintillation counting). AMS, unique to LLNL, is an ultra-sensitive analytical technique used for the quantification of long-lived radionuclides at ultra-low concentrations. Like other mass spectrometric techniques, AMS involves the counting of ions. The unique feature of AMS is the stripper canal used in a tandem accelerator, which effectively breaks all molecular bonds. Thus, AMS eliminates the molecular isobaric interferences (*e.g.*, ^{239}Pu versus ^{238}UH) that limit the sensitivity of conventional ICP-MS. The Center for AMS (CAMS) heavy-isotope system routinely achieves instrumental backgrounds of 10^5 atoms for actinide elements.

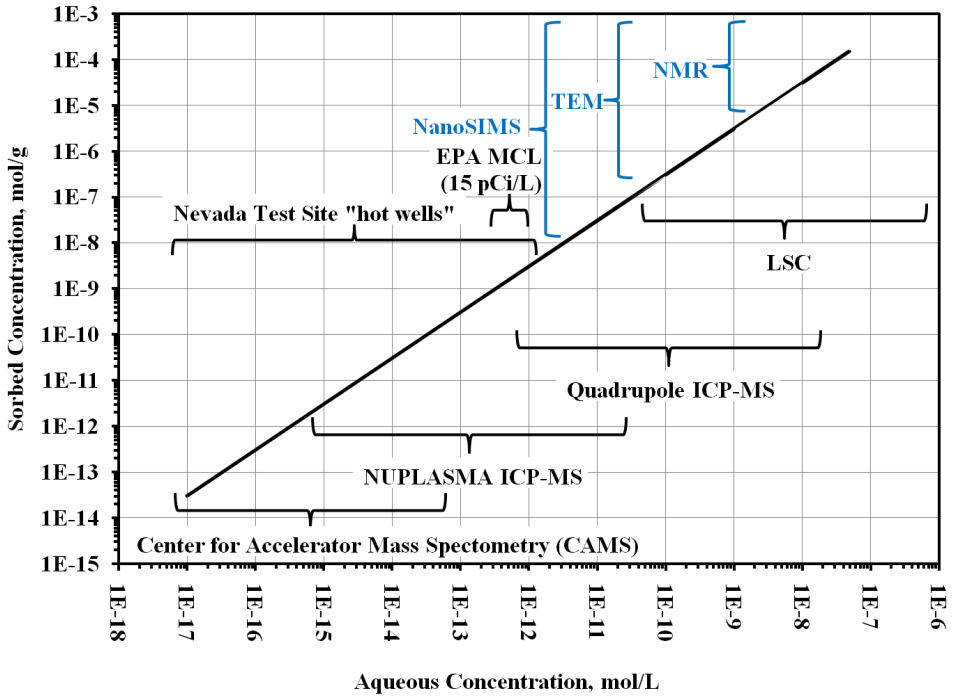

Figure A1. Predicted sorption behavior of Pu to goethite and its relationship to Pu concentrations observed in the field, EPA Maximum Contaminant Level (total alpha), and approximate detection ranges of various quantification and imaging techniques (based on typical Pu isotopes and sample prep. methodologies employed at LLNL).

The sorption isotherms produced in these experiments provide a unique opportunity to examine the sorption behavior from micromolar and to near attomolar Pu concentrations (Figures A2 and A3). Over a two week experimental time-frame, the Pu(IV) sorption isotherm at aqueous Pu concentrations ranging from $<10^{-16}$ to 10^{-9} M is linear, suggesting equivalent Pu sorption affinities to goethite over 7 orders of magnitude of surface loading. Under the controlled binary system conditions examined here, Pu(IV) sorption behavior at environmental (femtomolar) concentrations is, thus, not quantitatively different from behavior at nanomolar concentrations. Whether this conclusion holds true over a wider range of solution conditions (e.g. ternary systems) reaction times, and mineral phases is the subject of future research within this program. At concentrations $>10^{-9}$ M, Pu(IV) "sorption" does not reach equilibrium within a 7-day experiment. The behavior can be attributed to relatively slow nucleation of Pu precipitates. Homogeneous nucleation rates should increase with concentration due to an increasing thermodynamic driving force. However, surface catalyzed nucleation is limited by the access to surface sites at these concentrations.

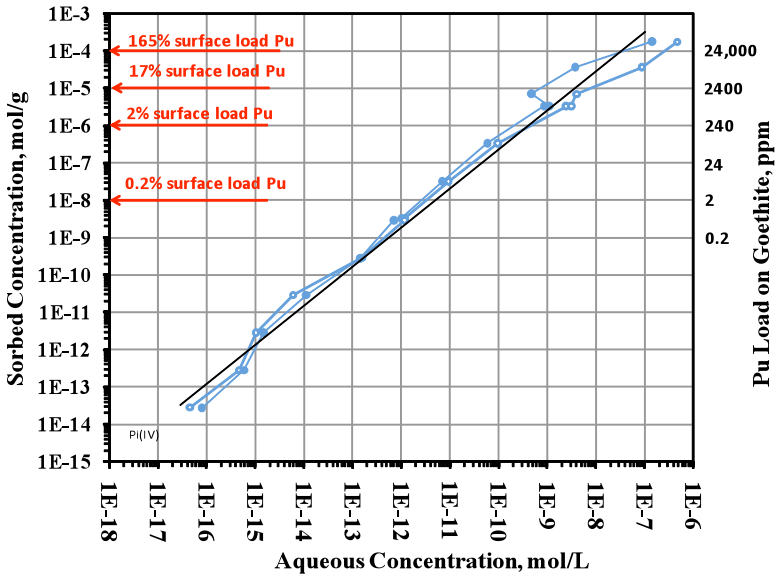

Figure A2. Pu(IV) sorption to goethite at 7 days (open circles) and 14 days (closed circles). Surface loading estimated base on surface area measurement and site concentration of 2.31 sites/nm^2 (DZOMBACK AND MOREL, 1990).

The sorption behavior of Pu(V) follows closely that of Pu(IV). Surface-catalyzed Pu(V) reduction to Pu(IV) on the goethite surface has been well documented (e.g. POWELL et. al., 2005) and can explain the apparently similar sorption behavior of the two Pu oxidation states. On the scale of weeks, the initial oxidation state of Pu in the aqueous phase no longer plays a significant role in the resulting sorption patterns, particularly at aqueous concentrations below 10^{-9} M. It is apparent that a steady state is reached in which Pu(IV) is the dominant oxidation state on the surface irrespective of the initial Pu oxidation state in solution. Rates of Pu "sorption" above 10^{-9} M appear to be generally slower for Pu(V) than Pu(IV) and can most likely be attributed to the limited surface sites available for surface catalyzed Pu(V) reduction at high concentrations. Additional data and discussion of surface catalyzed Pu polymerization and sorption are presented in the Appendix.

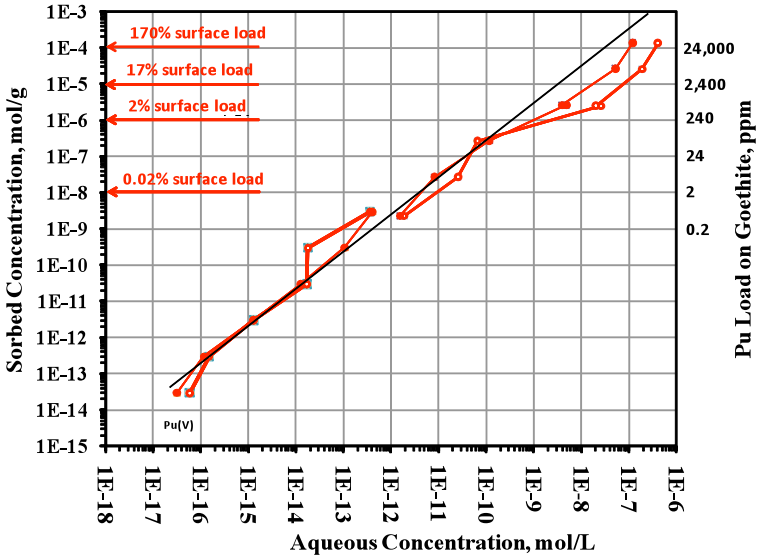

Figure A3. Pu(V) sorption to goethite at 7 days (open circles) and 14 days (closed circles). Surface loading estimated base on surface area measurement and site concentration of 2.31 sites/nm^2 (DZOMBACK AND MOREL, 1990).

Additional kinetic analysis of the Pu(IV) and Pu(V) sorption to goethite are presented in the Appendix.

Task A2: Determining the Lower Limits of our Experimental Capabilities

Our efforts to measure Pu at ultra-trace levels using CAMS were successful. Given the sample size of 100 mL used in isotherm experiments (Task A2), quantifying an aqueous Pu concentration of 5×10^{-17} M is equivalent to the detection of 3×10^{6} atoms. In fact, sample blanks indicate that quantitative measurement could be performed well below these concentrations, consistent with reported instrument backgrounds of 10^{5} atoms. In Figures A3 and A4 the deviation from linearity at the lowest concentrations can be attributed to slight background contamination during sample preparation. Pu-goethite experiments show that experiments would need to be conducted under more controlled clean-room conditions to maximize the resolving power of Pu AMS at low concentrations. LLNL is constructing a clean-room facility to allow measurements to 10^{-18}M.

Our efforts to determine the lowest detectable Pu concentrations using the NanoSIMS were also successful. Complementary TEM results are reported in Program Element C: Surface Precipitation of Pu Polymers.

While TEM exhibits atomic scale resolution, it is exceedingly difficult to resolve a monomeric distribution of atoms on a minerals surface, effectively resulting in a high detection limit (~100 ppm in the case of Task A binary Pu sorption experiments with goethite). This is in contrast to nanoSIMS whose spatial resolution is lower than TEM (50 to 500 nm, depending on analytical parameters) but whose detection limits were estimated on the order of 200 atoms for Pu. NanoSIMS of Pu-goethite sorption samples detected bulk Pu concentrations as low as 0.7 ppm, substantially lower than previously estimated (Figure A5). However, individual nano-colloids could not be resolved. TEM and nanoSIMS results, when combined with the uniform sorption affinities observed in 10^{-9} to $<10^{-16}$ M equilibrated samples (70 to 10^{-5} ppm on goethite) suggest that Pu sorption transitions from a nanocolloid surface precipitate to a more diffuse sorption behavior at approximately 70 ppm Pu on the goethite surface (or 10^{-10} M aqueous concentration). X-ray absorption spectroscopy will be pursued in FY11 to complement these techniques and further our understanding of spatial distribution and polymerization behavior of Pu. Additional information on the NanoSIMS can also be found in the Appendix.

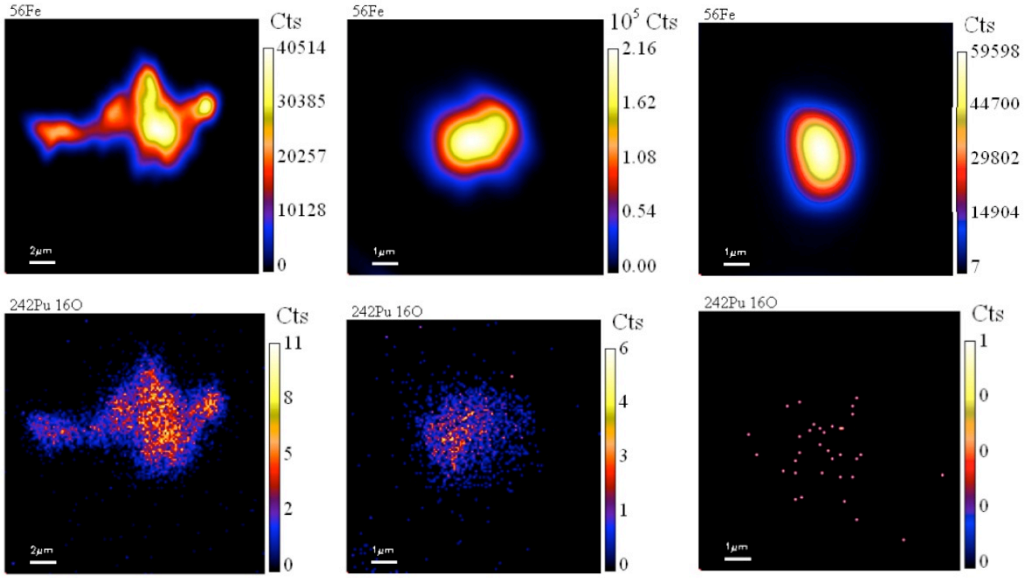

Figure A5. NanoSIMS images of 70 ppm Pu(V), 7 ppm Pu(IV), and 0.7 ppm Pu(IV) on goethite.

While TEM exhibits atomic scale resolution, it is exceedingly difficult to resolve a monomeric distribution of atoms on a minerals surface, effectively resulting in a high detection limit (~100 ppm in the case of Task A binary Pu sorption experiments with goethite). This is in contrast to nanoSIMS whose spatial resolution is far worse than TEM (50 to 500 nm, depending on the sputtering ion, current, and other factors) but whose detection limits were previously estimated to be on the order of 200 atoms for Pu. NanoSIMS analysis of Pu-goethite sorption samples was able to detect Pu on goethite in samples as low as 0.7 ppm, substantially lower than previously estimated (Figure A6).

However, individual nano-colloids could not be resolved. Nevertheless, the TEM and nanoSIMS results, when combined with the uniform sorption affinities observed in 10^{-9} to $<10^{-16}$ M equilibrated samples (70 to 10^{-5} ppm on goethite) suggest that Pu sorption transitions from a nanocolloid surface precipitate to a more diffuse sorption behavior at approximately 70 ppm Pu on the goethite surface (or 10^{-10} M aqueous concentration). X-ray absorption spectroscopy will be pursued in FY11 to quantitatively establish the point of transition to monomeric Pu adsorptive behavior.

Program Element B: Stabilization of Pu Surface Complexes on Mineral Colloids by Natural Organic Matter

(B. Powell: lead; Ruth Tinnacher, Students: L. Simpkin, T. Zimmerman and J. Jablonski)

The focus of Program Element B is to examine the influence of natural organic matter (NOM) on Pu sorption to pure mineral phases and sediments. The task is guided by the hypothesis:

> *NOM can increase Pu mobility by 1) forming NOM coatings on colloids which stabilize Pu surface complexes and 2) formation of aqueous Pu-NOM complexes which prevent sorption of Pu and increase subsurface mobility.*

The research plan consists of four tasks; the first two focus on equilibria of Pu-NOM (binary systems) and Pu-NOM-mineral (ternary systems) interactions. There is a strong coupling of these tasks with the binary (Pu-mineral) studies described in Program Element A.

Our FY10 milestone was to examine the influence of various NOM fractions on Pu sorption to model minerals. We have met this milestone with a series of screening experiments examining a set of reference NOM ligands to determine which ones influence Pu sorption to pure mineral phases (Task B1). These experiments have focused on Pu sorption to gibbsite in the presence of NOM surrogates such as Leonardite humic acid, Suwannee River fulvic acid, desferroxamine-B (DFOB), and citric acid. In addition, we have also determined stability complexes for actinide-humic acid complexation and are beginning studies examining actinide-fulvic acid complexation (Task B2). These activities were initially slated for year 2 but it was decided the thermodynamic data would be useful in interpreting results from Task B1.

Task B1: Screening for Enhanced Pu Mobilization by NOM

The objective of this task is to examine representative NOM surrogates (citric acid, desferroxamine-B, extracellular polymeric substances, fulvic acid, and humic acid) to determine their influence on Pu sorption to minerals and sediments. To date our experiments have focused on Pu sorption to gibbsite ($Al(OH)_3$). This has allowed the research group to take advantage of a surface complexation database previously developed by the Clemson research team (POWELL et al., 2008). A new source of gibbsite was used in these experiments so a representative sorption edge was generated for Pu(IV) and Pu(V) to compare with the previous data. The new sorption edge is shown in the Appendix and is consistent with previous data.

Influence of humic acid (HA) on Pu sorption to gibbsite

The influence of HA on Pu sorption to gibbsite was examined in a set of batch sorption experiments. Distribution coefficients (K_d) that measure the ratio of the Pu concentration on the solid phase versus the Pu concentration in the aqueous phase were 1000 L/kg and 2000 L/kg for Pu in the absence of HA at pH 4 and 6, respectively. In the presence of HA, the distribution coefficients increased to 14,500 L/kg and 22,500 L/kg at pH 4 and 6, respectively. The phenomenon identified in these experiments indicates that HA under these pH conditions may enhance colloid-facilitated transport (stabilization of Pu-colloid association) and/or inhibit Pu transport (stabilize Pu association with sediments) depending on identity and abundance of mineral phases.

Influence of fulvic acid (FA) on Pu sorption to gibbsite

Fulvic acid is expected to have relatively similar functional groups as HA but represents a lower molecular weight fraction of NOM. Therefore, a series of experiments were set up to determine the effect FA would have

on plutonium sorption to gibbsite. A set of solid-free control samples were prepared and analyzed simultaneously. Samples were analyzed at 1, 7, and 33 days; steady state had been achieved by the 7th day (Figure B1). Fulvic acid was added to the samples to achieve total concentrations of 1, 5.5, and 50.5 mg/L. Samples were adjusted to pH 4, 6, 8, and 10, and all samples were prepared in duplicate, excluding the solid-free controls.

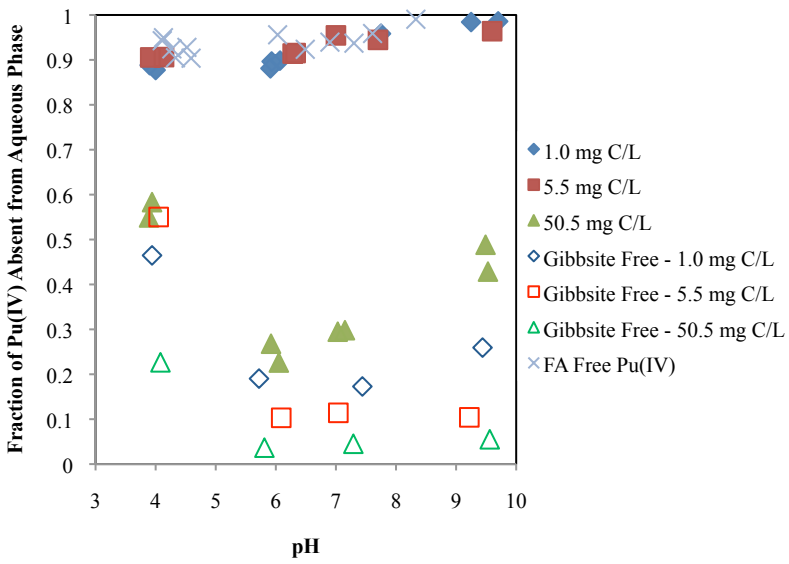

Figure B1: Plot showing the fraction of Pu(IV) absent from the aqueous phase in ternary system batch sorption experiments as a function of pH. The concentration of Pu(IV) was 10^{-10} M, gibbsite concentration was 5 g/L, NaCl was 10 mM and fulvic acid was 1.0, 5.5, or 50.5 mg/L. Samples were mixed continuously then aliquots were removed for analysis after 1, 7, and 33 days. Data shown are from the 7th day sampling event. Samples were passed through 30k MWCO centrifugal filters and the Pu concentration in the filtrate was determined using liquid scintillation counting (LSC).

Previous experiments have shown nearly complete sorption of Pu(IV) to the mineral phase in ligand-free systems above pH 4 (Appendix, POWELL et al., 2008). The data presented in Figure B1 shows that the presence of FA causes an increase in aqueous Pu concentrations relative to FA free systems. The most significant difference can be observed in the 50 mg-FA/L dataset where the aqueous phase concentration of Pu is significantly higher than FA free systems. There is a slight increase in the fraction of aqueous Pu with increasing FA concentration indicating that the presence of fulvic acid prevents Pu sorption. This is attributed to formation of stable aqueous Pu-FA complexes. Across the pH range 5-9, Pu sorption increases with increasing pH. In this region, the mineral surface carries a net negative charge resulting in competition between the FA and the surface for complexation/sorption of Pu(IV). Conversely, sorption of FA to gibbsite decreases with increasing pH. This is consistent with anionic functional groups of the FA interacting with positively charged gibbsite sites at low pH and being repelled by negatively charged sites at high pH.

It was expected that in the solid-free control samples, all Pu(IV) would remain in the aqueous phase. However, Figure B2 shows this was not necessarily the case, particularly at low pH values. Also, as in the samples containing gibbsite, a larger concentration of FA leads to more Pu(IV) remaining in the aqueous phase. The loss of Pu(IV) from the aqueous phase in solid-free control samples may be attributed to sorption to the vial walls, precipitation, or filtration. To monitor possible sorption to the vial walls, at the end of the experiments the vial contents were rinsed out and 0.1 M NaOH was used to leach Pu-FA complexes from the walls. Between 1 and 25 % of the total Pu was found to be associated with the vial walls in solid-free control samples and between 0.5 and 15% for the samples with gibbsite present. Competition between the vial walls and mineral surfaces for sorption of Pu and Pu-FA complexes is present. Therefore, the fraction lost from the aqueous phase in the solid-free samples cannot be simply subtracted from the samples containing gibbsite, as competition between the mineral surface and the vial walls will exist in that system. Mass balance calculations of Pu in the gibbsite free systems indicated some loss of Pu at low pH values and low FA concentrations (data in Appendix). Therefore, removal of some Pu *via* filtration could be occurring in these systems and requires further study.

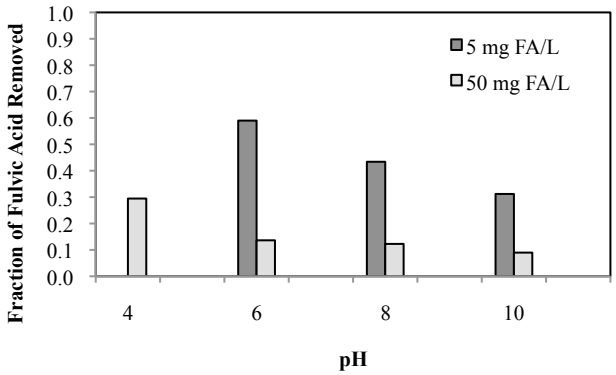

Figure B2: Fraction of FA absent from the aqueous phase in the presence of gibbsite. Fulvic acid may have been removed due to sorption to gibbsite, aggregation, or by the filtration step. Samples were prepared containing gibbsite at 5 g/L in 0.1 M NaCl. Samples were at 1, 7, and 33 days; data are from the 7th day sampling event. Samples were passed through 30k MWCO centrifugal filters and the fulvic acid concentration in the filtrate was determined using UV-Vis spectroscopy.

The complex behavior of Pu in the presence of FA is hypothesized to be the result of Pu interacting with various fractions of the FA. Fulvic acids and HA do not have a fixed structure, rather they are a mixture of low and high molecular weight organic compounds with phenolic and carboxylic functional groups. Fractionation of FA in the presence of mineral surfaces has been frequently observed in previous studies. Generally, the low molecular weight hydrophilic fraction remains in solution and the higher molecular weight hydrophobic fractions associate with mineral surfaces (DAVIS AND GLOOR, 1981). This behavior may help to explain the differences between the influence of HA and FA on Pu sorption. The HA may contain a larger, high molecular weight fraction that will complex Pu and preferentially partition to the mineral surface under low pH conditions (as observed for the pH 4 and pH 6 partitioning data). Conversely, the more hydrophobic FA fractions may complex Pu and remain in the aqueous phase.

Plutonium forms strong, stable aqueous complexes with FA. However, no data are available for Pu-FA stability constants. Experiments have been set up to determine Pu(IV)-FA stability constants using the discrete pKa model described above. However, an ultrafiltration separation technique cannot be used due to incomplete removal of the FA with filtration as required by the method. Therefore, future solubility experiments will be performed using Pu(IV) nanoparticles across the pH range 3-9. Characterization of the Pu nanoparticles will be determined through scanning electron microscopy and transmission electron microscopy using a similar approach to that being used in Program Element C. Samples containing the Pu(IV) nanoparticles will be amended with FA and the solubilization of Pu by formation of Pu-FA complexes will be monitored using inductively coupled plasma mass spectrometry (ICP-MS). The Pu-FA stability constants will be determined based on the increased solubility of Pu nanoparticles in the presence of FA.

Modeling efforts will be undertaken in FY11 to predict the sorption data by combining the aqueous speciation constants determined in this work and published surface complexation constants (POWELL et al., 2008). Ongoing studies with Pu-citric acid-gibbsite systems for which Pu-citric acid aqueous complexation constants are available indicate that the combination of the binary (ligand-Pu and mineral-Pu) thermodynamic constants can successfully predict the sorption behavior observed in batch tests.

Task B2: Determination of Stability Constants for Relevant Pu-NOM Complex

Task B2 is focused on verifying and enhancing existing thermodynamic data for Pu-NOM complexation. Data for actinide binding to NOM are sparse. However, in order to quantify the fate and transport of Pu in subsurface environments, reliable aqueous complexation data are required. In this task, we modified a traditional equilibrium dialysis ligand exchange technique (VAN LOON *et al.*, 1992) for use with standard ultrafiltration devices to determine aqueous actinide-humic acid stability constants. A detailed description of this work is provided in Zimmerman (2010; MS Thesis, Clemson University) and an extended abstract are in the Appendix. Leonardite humic acid (HA) from the International Humic Substance Society was used as a model humic acid (HA). The binding of actinides to HA was modeled using a discrete ligand binding approach assuming constant proton binding constants listed in Table B1.

Table B1: Stability constants determined for actinide binding with Leonardite humic acid in 0.1M NaCl.

Reaction	Stability Constant
$HL1 \leftrightarrow H^+ + L1^-$	pKa = 3
$HL2 \leftrightarrow H^+ + L2^-$	pKa = 5
$HL3 \leftrightarrow H^+ + L3^-$	pKa = 7
$HL4 \leftrightarrow H^+ + L4^-$	pKa = 9
$Pu^{4+} + HL3 + 2H_2O \leftrightarrow Pu(OH)_2L3^+ + 3H^+$	log K = 6.76
$Th^{4+} + HL3 + 2H_2O \leftrightarrow Th(OH)_2L3^+ + 3H^+$	log K = 3.58
$NpO_2^+ + HL1 <=> NpO_2L1 + H^+$	log K = 0.31
$NpO_2^+ + HL2 <=> NpO_2L2 + H^+$	log K = -1.35
$NpO_2^+ + HL3 <=> NpO_2L3 + H^+$	log K = -2.28

The actinide complexation reactions listed in Table B1 were determined from the experimental data in Figure B3. As expected tetravalent Th(IV) and Pu(IV) showed stronger affinity for HA than pentavalent Np(V). Allowing the Np(V) samples to equilibrate an additional 4 weeks did not significantly change the results indicating that little Np(V) reduction to Np(IV) occurs in these samples which are exposed to air. Furthermore, the binding constant for Np(V) can be used as a surrogate for Pu(V). The binding of Pu(IV) to HA is stronger than binding of Th(IV) to HA. This is consistent with Th(IV) and Pu(IV) binding to other ligands as shown by a standard linear free energy relationship (see Appendix). These stability constants can be used for predicting aqueous speciation of the actinides. This will be particularly important when deconvoluting the influence of NOM on Pu sorption to minerals and sediments.

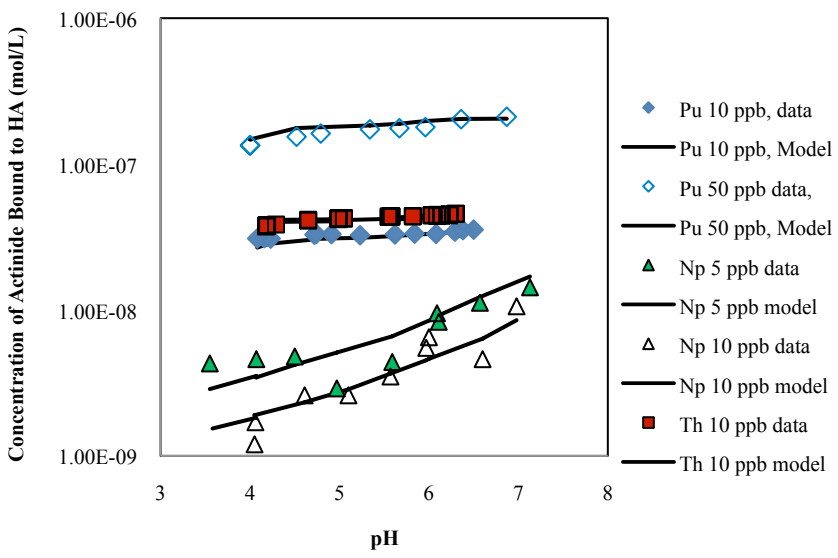

Figure B3: Actinide binding to Leonardite humic acid. Th(IV) and Pu(IV) data are shown after 10 days of equilibration in 0.1 M NaCl, 0.01 M EDTA background solution. EDTA was present as a reference ligand to prevent Pu(IV) precipitation. Np(V) data are shown after 24 hours of equilibration in 0.1 M NaCl. No reference ligand was required for Np(V) studies due to inherently high solubility of pentavalent actinides. Total concentrations of each actinide under experimental conditions are listed within legend. Solid lines are model fits using equations listed in Table B1.

Program Element C: Surface Precipitation of Pu Polymers: Experimental and Natural Nanocolloids

(A. Kersting: lead; B. Powell, Z. Dai, R. Kips, and P. Zhao)

The focus of Program Element C is to characterize the conditions under which Pu sorbs as a precipitate *versus* when it sorbs as monomeric surface complex. A second objective is to understand how our experimental

findings compare with *natural* colloids contaminated with Pu at several field sites. This Program Element is strongly integrated with Program Elements A, B D and E. We are testing the following hypothesis:

> *The apparent sorption/desorption of Pu to mineral colloids is the result of surface precipitation of pure Pu nanopolymers. The stability/solubility of the Pu polymers will be affected by their depositional characteristics and interaction with the mineral surface.*

The low solubility of Pu(IV(must be considered in any interpretation of laboratory sorption experiments conducted at relatively high concentrations (>10^{-9} M) that could likely result in precipitation of PuO_2 polymer as a result of oversaturated solution conditions. Recent work by Neck *et al*. (NECK et al., 2007) and Soderholm *et al*. (SODERHOLM et al., 2008) sheds light on previously conflicting Pu(IV) solubility studies, suggesting that aqueous Pu(V) and 2- to 20-nm Pu colloids are expected to be present in solution. Thus, most laboratory Pu "sorption" experiments carried out at Pu concentrations greater than 10^{-9} M Pu(IV) should, in fact, be regarded as reflecting adsorption of Pu in multiple oxidation states and the interaction of polymeric Pu(IV) clusters with mineral surfaces.

In FY10 our experimental milestones were to finish our preliminary investigation of the structure of Pu(IV) colloids on goethite and silica and expand this effort to include Pu(V) (Task C1). Of particular interest is understanding what surface loading and aqueous concentrations results in incipient Pu polymerization at high Pu concentrations. An additional milestone was to initiate external collaborations to investigate natural colloids samples from a contaminated DOE site (Task C2). We completed all our milestones and started one additional collaboration involving examination of samples from Russia. The results of the first part of Task C1 were written up in manuscirpt form and recently submitted to *Environmental Science & Technology*. For Task C2, samples from Hanford Reservation were analyzed by SEM and NanoSIMS as part of a new collabration with Andy Felmy at (PNNL). In addition, aquifer solids from Tomsk, Russia, a radionuclide waste injection site, were analysed as a result of a new collaboration with Stepan Kalmykov at Moscow State University.

Task C1: Experimental Determination of Monomeric Versus Polymeric Pu Precipitation

Experimental studies focused on characterizing the chemical form of Pu on mineral surfaces. Particular emphasis was placed on identifying Pu concentrations and solution conditions that result in the formation of Pu polymers. In one study, the nanostructure of Pu colloids was investigated using high-resolution TEM for four different samples; 1) intrinsic Pu nano-colloids, 2) intrinsic Pu nano-colloids added to goethite colloids, 3) dissolved Pu(IV) added incrementally to goethite, and 4) dissolved Pu(IV) added incrementally to quartz.

Intrinsic Pu nano-colloids that were formed were 2-5 nm in diameter, and both electron diffraction analysis and HRTEM confirm the expected *Fm3m* space group with the fcc, PuO_2 structure. In the experiment in which intrinsic Pu nano-colloids were formed first and then mixed with goethite colloids, the majority of the Pu nano-colloids did not associate with goethite, but instead remained as colloid nanoclusters captured on the carbon film of the TEM grid. High-resolution TEM imaging (Fig. C1) and FFT analysis of the intrinsic Pu nano-colloids retained the same *fcc* PuO_2 structure as the original intrinsic Pu nano-colloids. In contrast, Pu nano-colloids formed by incrementally adding a dissolved Pu(IV) solution to a goethite suspension formed 2-5 nm nanoclusters on the mineral surface (Fig. C2). High-resolution imaging and electron diffraction analysis show that these nanoclusters do **not** have the expected *Fm3m* space group, but rather the *Ia3* space group, matching the bcc Pu_4O_7 structure.

The plutonium nano-colloids that formed on goethite have undergone a lattice distortion relative to the ideal fluorite-type structure, fcc, PuO_2, resulting in the formation of a bcc, Pu_4O_7 structure. This structural distortion results from an epitaxial growth of the plutonium colloid on goethite, resulting in a stronger binding of plutonium to goethite compared with other minerals such as quartz for which this distortion was not observed. This finding provides new insight for understanding how molecular-scale behavior at the mineral-water interface may facilitate transport of plutonium at the field scale.

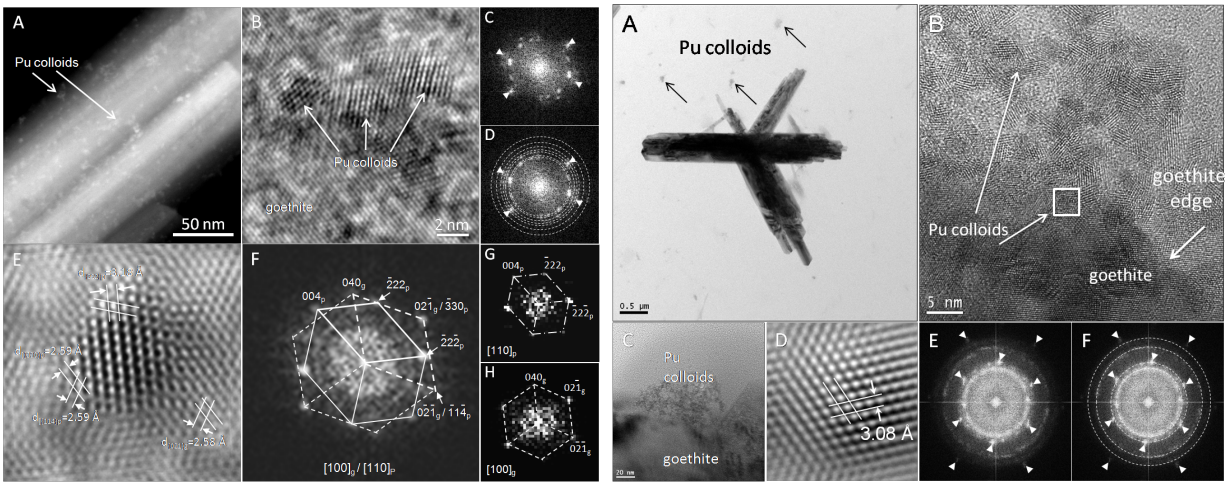

Figures C1 and C2. The composite figure, C1, on the left shows Pu_4O_7 nano-colloids formed *in situ* on goethite. The second composite figure, C2, on the right shows Pu colloids located off the goethite crystal with the expected the fcc, PuO_2 structure.

Task C2: Characterization of Pu-Colloid Interfaces on Natural Colloids

The objective of this task was to determine the form of the Pu found on environmental samples. We initiated a collaboration with Andy Felmy at PNNL, to characterize a series of highly contaminated soil samples collected beneath a Hanford crib in an effort to determine how Pu is associated with the subsurface mineralogy. This project is quite challenging as concentrations are usually below detection limits, but if successful will help to better understand how the Pu has been transported under a given set of geologic conditions.

Hanford Reservation, Washington State

Throughout its history as a plutonium production site to the U.S. nuclear weapon program, direct discharges and leaks of transuranic liquid waste have resulted in both soil and groundwater contamination at and around the Hanford site. In some cases, transuranic radionuclides were co-disposed with acidic liquid waste, resulting in transport through the vadose zone for considerable distances.

We received a set of historical samples from three different depths beneath a crib at the Hanford Reservation. These samples contained approximately 5 grams of sand/silt soils collected at depths 49 - 64 ft beneath the surface. An overview of the samples and their activity for ^{241}Pu, ^{239}Pu and ^{241}Am, as measured by gamma spectroscopy, is given in Table C1.

Table C1. Hanford soil samples

Sample ID	depth	soil (g)	Am-241 (nCi)	Pu-241 (nCi)	Pu-239 (nCi)
B1HVC8	49-50'	5.96	152	below DL	45
B1HK15	63.5-64.5'	5.38	344	1516	382
B1HY61	**> 65'**	5.53	125	36	134

Several milligrams of sample were embedded in epoxy, polished, stored in an inert atmosphere and finally carbon-coated for analysis by scanning electron microscopy (SEM) and NanoSIMS. SEM images of B1HK15 #1 showed many exposed mineral surfaces of different elemental composition (Fig. C3). Backscattered electron imaging (for compositional contrast) in combination with energy-dispersive X-ray analysis (EDX) identified Si, O, Al, Mg, Ca and Fe as the main constituents of this soil sample, with 'hot spots' of Ba and Ti. For the other samples (B1HY61, B1HVC8) the EDX spectra also showed S as a high abundant element in some locations.

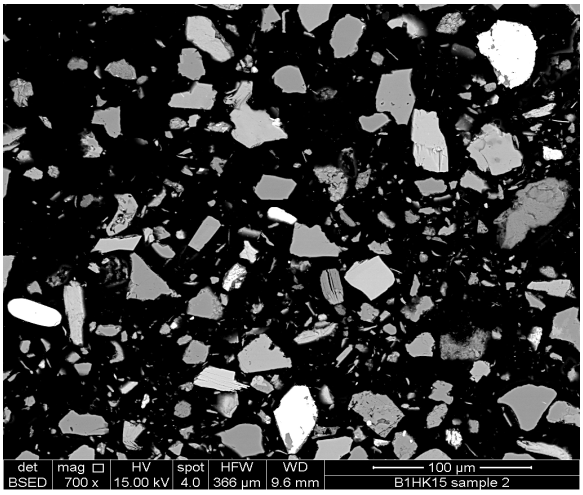

Figure C3. SEM image (mag 700×) of the backscattered electrons from a Hanford soil sample (B1HK15) embedded in epoxy. The brighter the pixel, the higher the atomic (Z) number of the mineral.

Sample B1HK15 and B1HY61 had the highest activity according to gamma spectroscopy measurements (Table C1) and were therefore selected for initial analyses. The ^{239}Pu isotope should in fact be a factor 50-60 more abundant than the combined ^{241}Pu and ^{241}Am isotopes, based on their specific activity. Since no similar goethite standard was at hand for ^{239}Pu, the mass calibration was verified using the $^{238}U^{1}H$ (uranium hydride) from a uranium oxide sample. The set of standards developed for use on the NanoSIMS were previously presented in Program Element A, Task A2 and are not repeated here. A more detailed description of the NanoSIMS analysis protocol is given in the Appendix.

An array of fourteen 30 x 30 µm ion images, each collected at different locations on sample B1HK15 #2, was collected in multi-collection mode. Our initial analyses suggest that Pu, although low in concentration, can be detected in this sample. For only 2 of the 14 areas analyzed significant counts at mass 239 and 255 (for $^{239}Pu^{16}O$) were detected. Fig. C4 shows an area where the mass 239 and mass 255 counts were mainly located near the edges of the grains. Note that the count rates for ^{27}Al and ^{40}Ca were also very high in these regions.

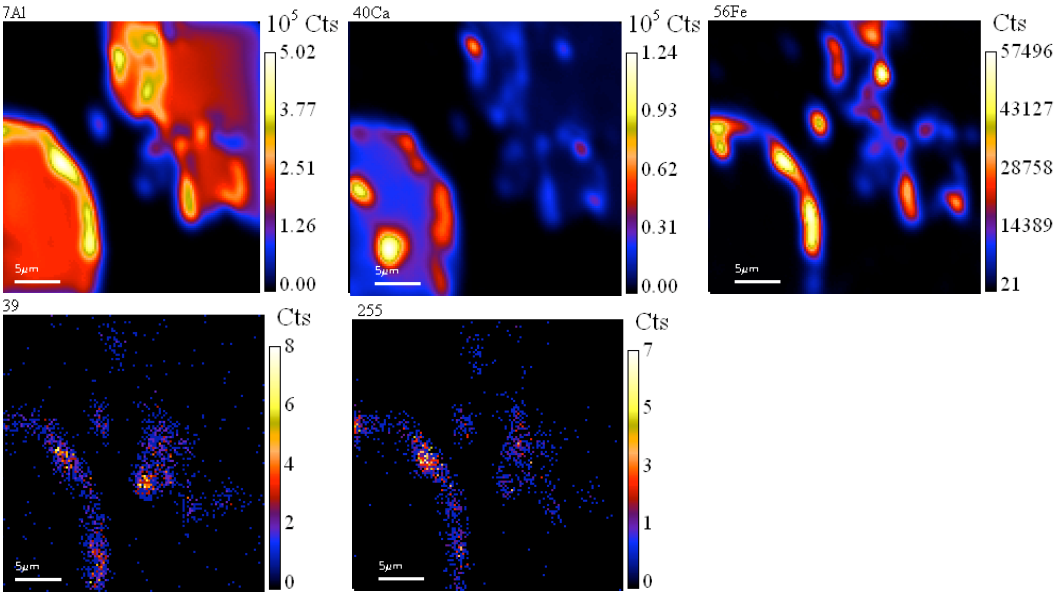

Figure. C4. 30 x 30 µm ion images of ^{27}Al, ^{40}Ca, ^{56}Fe, mass 239 (attributed to ^{239}Pu) and mass 255 (attributed to $^{239}Pu^{16}O$) showing increased secondary ion counts for mass 239 and mass 255 near the edges of the grains.

A second array of 14 ion images was collected on sample B1HK15 #2, showing a similar correspondence between Pu and Fe. Results are in the Appendix. A final set of measurements on sample B1HY61 #1 showed similar results: significant mass 239 and mass 255 counts were collected in 5 out of 12 ion images, of which 2 showed some correlation with the ^{56}Fe ion image. The counts for mass 241 and mass 257 (=241 + ^{16}O) were also collected, but these did not exceed background. No figures are shown.

We caution that these are preliminary results and both ion species showed detectable, but low and fairly stable count rate throughout the analysis. The possibility of unresolved mass interferences needs to be taken into account, especially for mineral samples in which a wide range of elements is present. We are exercising caution in the interpretation of these ion images, and need to combine this information with data from other analytical techniques such as Transmission Electron Microscopy (TEM) and Electron Microprobe X-ray analysis. Efforts in FY11 will continue with analyses of these samples.

Tomsk, Russia

Another environmental soil sample, prepared as a carbon-coated thin section, was provided to us by Dr. S. Kalmykov who collected samples at a drilling point several kilometers down gradient of the Siberian Group Chemical Enterprises site near the town of Tomsk, Russia. The thin section was prepared from drill-core cuttings collected within the main aquifer, approximately 500 m away from the original injection site. This site was contaminated with actinides and transuranic liquid waste over tens of years.

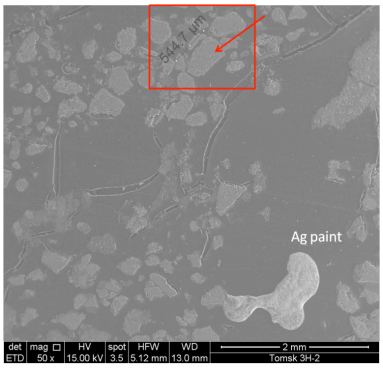

Fig. C5. SEM image (mag 50×) of the grain of interest (red box) for NanoSIMS analysis. Silver paint was used for relocation.

A solid-phase sample was measured by alpha-radiography, and showed an increased number of alpha tracks near the edges of a 500 µm grain (Fig. C5). EDX mapping identified 'hot spots' of Fe near the edges as well. The location of the grain was labeled with Ag paint for relocation on the NanoSIMS. NanoSIMS analyses on this grain showed counts for mass 254 (attributed to ^{238}UO), but nothing above background for masses 239, 241, 242, 251 (^{235}U^{16}O) and 255 (Figure C6). Note that the U is correlated with the oxidized edge of the grains where the alpha-radiography tracks are the most concentrated.

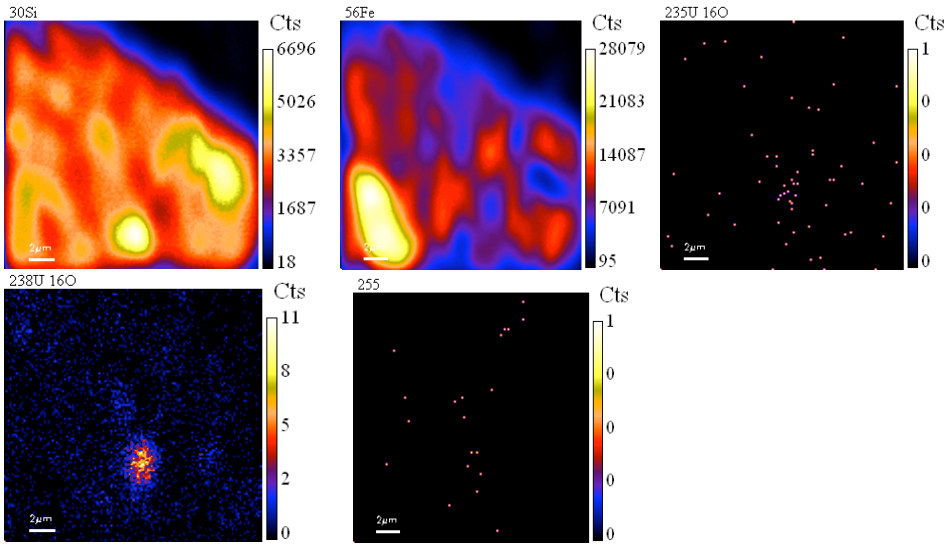

Figure C6. 20 x 20 µm ion images of ^{30}Si, ^{56}Fe, mass 251 (attributed to ^{235}UO), mass 254 (attributed to ^{238}UO) and mass 255 for the Tomsk grain.

In contrast to what we expected, the mass 239 counts were in several cases higher than the mass 255 counts, with a 239/255 ratio varying between 0.7 and 4.1. The probability of (irresolvable) mass interferences should be

considered here, and therefore combining the data from the NanoSIMS ion images with information from complementary analytical techniques such as Transmission Electron Microscopy (TEM) and Electron Microprobe X-ray analysis is the next step. We will expand our standard library to include samples for all the isotopes of Pu. For our future experiments, we plan to continue the NanoSIMS measurements on these environmental soil samples, while further improving the accuracy and reliability of the data through the use of a goethite standard amended with 50-70 ppm of ^{239}Pu. With X-ray diffraction we hope to obtain information on the mineralogy of the soil samples, which will help to correlate the Pu counts detected in the NanoSIMS with the different mineral phases.

Program Element D: Co-precipitation with Altered Colloids

(S. Carroll: lead; Patrick Huang, Harris Mason and M. Zavarin)

At the NTS, 98% of the Pu and other actinides deposited in the subsurface as a result of an underground nuclear test is predicted to be sequestered by melt glass produced as a result of the extreme temperatures associated with a nuclear detonation. This Program Element is designed to investigate the Pu solubility and structure when the Pu is associated with colloidal silicates and nuclear melt glass from the NTS. Experiments conducted in this element will determine the conditions under which dissolved Pu concentrations are controlled by isomorphic substitution in secondary phases and those under which they are controlled by PuO_2 solubility (even at low concentrations). The hypothesis guiding the effort in Program D is the following:

> *Colloid formation during primary rock alteration and secondary mineral precipitation can structurally isolate Pu in colloids at environmental concentrations*.

This Program Element consists of three tasks. Task D1 is designed to model the sorption of Pu at the silica/water interface at environmental concentrations. Given the difficulties in the experimental analysis of Pu sorption and co-precipitation at environmental concentrations, atomic-scale simulations are essential to clarify the nature of Pu aqueous speciation, sorption at mineral/water interfaces, and incorporation into the mineral framework. Task D2 involves using NMR and solution chemistry to probe the structural environment of Pu with inorganic, organic and microbial colloids. Task D3 is a series of experiments that alter and characterize nuclear melt glass from the NTS.

For FY10 our milestone was to begin molecular-scale simulations taking advantage of advances in algorithms and computing hardware at LLNL that allow for the finite-temperature simulation of simple interfaces that explicitly include a liquid water layer. We have carried out first principles molecular dynamics simulations for the a-Al_2O_3(0001)/water interface, and our findings for the interfacial structure are consistent with synchrotron X-ray scattering experiments (ENG et al., 2000).

Task D1: Molecular Scale Simulations

Benchmarking ab initio electronic structure methods for the accurate description of aqueous Pu(IV) complexes

At extremely low concentrations, there are no spectroscopic techniques that allow interrogation of the electronic structure of elements on mineral surfaces. Thus, we have embarked on a program of computational work employing a range of *ab initio* techniques including correlated wave function approaches (complete active space self-consistent field, CASSCF; multi-reference perturbation theory, MRPT) and density functional theory (DFT). We have also performed first-principles molecular dynamics within the DFT framework. Hardware resources available for this work include IBM BlueGene/L, currently ranked seventh on the TOP500 list of supercomputers. Figure D1 is a schematic organization of various *ab initio* methodologies in terms of computational cost versus accuracy. Note that model force fields, commonly used, are not *ab initio*. *Ab initio* methodologies, although employ increasing cost (e.g. computational time), provide enhanced accuracy.

In general, the electronic structure of actinide (An) complexes poses numerous difficulties. The high-*Z* elements exhibit large relativistic and spin-orbit coupling effects. The description of open-shell *f*-electrons is problematic due to strong correlation effects. Accurate treatment of actinide complexes often require sophisticated correlated

wave function techniques whose cost grows rapidly with the number of electrons, and thus are only practical for the small systems. To date, most of the theoretical works have focused on the actinyl complexes AnO_2^+ and AnO_2^{2+}, for which detailed experiments in gas and aqueous phases are available for comparison and validation.

Methodologies with lower computational effort are possible (Figure D1), but introduce uncontrolled approximations that require careful testing. The most common of these are based on DFT, which can potentially address larger and more complex systems. However, current approximations for exchange-correlation are not robust when applied to actinides. For example, DFT within the generalized gradient approximation (GGA) for solid PuO_2 oxide incorrectly yields a ground state that is metallic, when in fact it should be insulating. Hybrid functionals improve on this, giving the correct insulating ground state of solid PuO_2. On the other hand, for the PuO_2^{2+} and PuN_2 molecules, DFT-GGA predicts ground state structures and vibrational frequencies that are in good agreement with multi-reference perturbation theory, while hybrid functionals exhibit *worse* agreement compared to DFT-GGA. Thus, before continuing on any extensive *ab initio* simulations, we first carried out benchmark studies.

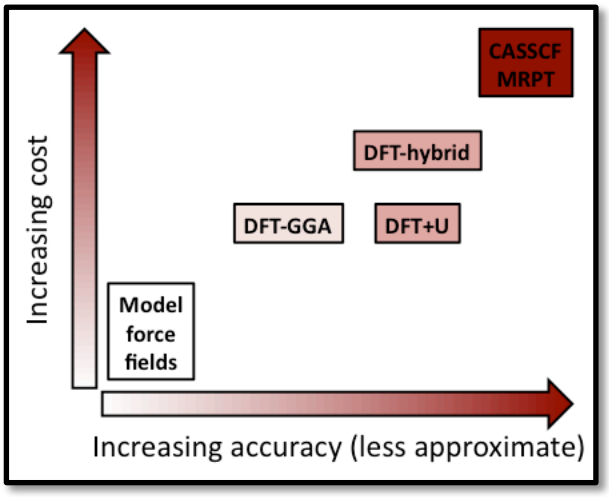

Figure D1: Schematic organization of various *ab initio* methodologies in terms of computational cost versus accuracy. Note that model force fields are not *ab initio*. Molecular dynamics with model force fields is commonly utilized for the simulation of aqueous geochemical systems; it is included here for comparison with the *ab initio* approaches that we employ in our work.

In FY10 we focused on benchmark studies looking at the $Pu(OH)_4$ molecule as a starting model for aqueous Pu(IV) at neutral pH. At pH values as low as ~ 1, Pu(IV) undergoes rapid hydrolysis to form $Pu(OH)_x^{4-x}$, which then continues to polymerize to form colloidal precipitates. Experimental characterizations to date have examined aqueous Pu(IV) well above its solubility limit (~ 10^{-13} to 10^{-15} M), and thus no information is available on the speciation of Pu(IV) at low concentrations and neutral pH under environmental conditions of interest. It is very possible that at low concentrations, Pu(IV) sorbs onto mineral surfaces as a monomer. In this case, *ab initio* methods are ideally suited to probe Pu(IV) speciation and reactivity under such conditions.

The isolated $Pu(OH)_4$ molecule is small enough to be treated with both high-level and more approximate methods, and is therefore a suitable test case for benchmarking electronic structure methods for Pu(IV). We consider two possible isomers of $Pu(OH)_4$: tetrahedral and planar. More details on the methodology employed can be found in the Appendix.

Our results for the tetrahedral and planar $Pu(OH)_4$ molecules are summarized in Table D1. All methods agree that the lowest energy structure for the isolated molecule is tetrahedral. There is general agreement that the planar isomer is a transition state (as determined by analysis of the Hessian matrix). The only exception to this is DFT-GGA, which finds that the planar structure is a local minimum, in qualitative disagreement with all the other methodologies. DFT-GGA also performs the most poorly for other properties; bond lengths are wrong by ~ 0.1 Å as compared to MRPT, and the energy difference between the tetrahedral and planar isomers is less than half the MRPT value. While the structural parameters are improved with DFT-hybrid, large errors remain in the barrier to the planar transition state. Problems with the DFT-based methods are also seen in the potential energy between $Pu(OH)_4$ and one water molecule, shown in Figures D2 and D3. The potential curves are calculated by bringing together $Pu(OH)_4$ and H_2O together, with the O in H_2O directed towards the Pu. The geometry within

each of the two monomers is held fixed while the Pu–O distance is varied. We find that the DFT-based methods underestimate water binding to $Pu(OH)_4$ by ~ 30% relative to MRPT.

	DFT-GGA	DFT-hybrid	CASSCF	MRPT
tetrahedral				
R(Pu–O) [Å]	2.17	2.11	2.10	2.08
R(O–H) [Å]	0.97	0.96	0.94	0.96
planar				
R(Pu–O) [Å]	2.20	2.14	2.13	2.11
R(O–H) [Å]	0.98	0.96	0.94	0.96
E(plan) – *E*(tet) [eV]	0.52	0.70	1.52	1.32

Table D1: Bond lengths (in Å) and energy difference (in eV) between the planar and tetrahedral isomers, at varying levels of ab initio theory. For DFT-GGA, the specific form employed here is the GGA due to Perdew, Becke, and Ernzerhof (PBE). DFT-hybrid refers to the hybrid extension of PBE, the PBE0 functional.

The errors in the DFT-based methods can originate from two possible sources: 1) the use of a single-reference theory to describe *f*-electrons that are multi-reference in character, or 2) the self-interaction error inherent in the DFT functionals. We rule out the first explanation above because the CASSCF converges to a wave function with a single dominant configuration. Using this single dominant configuration as reference for MP2 (a single-reference theory) yields excellent agreement with MRPT. Thus, a single-reference theory such as Kohn-Sham DFT should in principle be able to deliver accurate predictions for the ground state, provided that a good approximation for exchange-correlation is available.

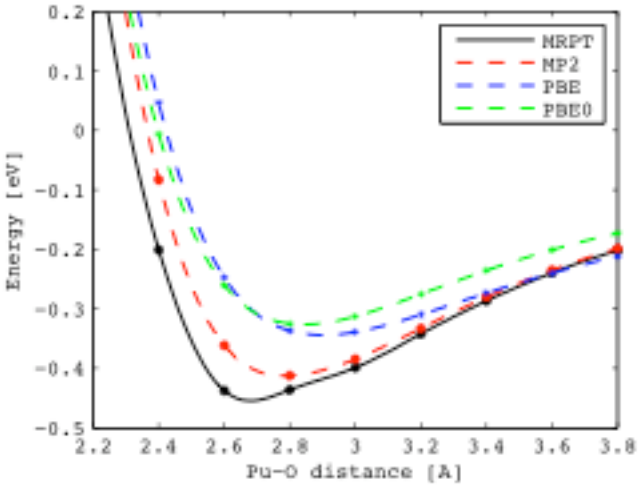

Figure D2: Tetrahedral $Pu(OH)_4 – H_2O$ potential energy. The water molecule is oriented with the O atom pointed towards Pu, with the water approaching $Pu(OH)_4$ along its three-fold axis of symmetry.

Unfortunately, *ab initio* dynamical simulations of condensed phases typically resort to DFT-GGA, which we have now shown to be inaccurate for Pu(IV) complexes. The errors from DFT-GGA arise from the poor description of the localized Pu *f*-electrons, a generally known problem with GGA functionals. Our work in FY10 suggests that a simple extension of the usual DFT-GGA method, DFT+U, can potentially correct the deficiencies in DFT-GGA. Current work now focuses on developing the DFT+U model for Pu(IV) complexes, and applying the technique to study Pu(IV) at the mineral/water interface.

Finally, note that the interaction of water to planar $Pu(OH)_4$ is quite strong (almost 1.5 eV), about three times stronger than the interaction with tetrahedral $Pu(OH)_4$. While the tetrahedral isomer is favored in the gas phase,

the strong water coordination to the planar isomer suggests that in an aqueous environment, the planar from can potentially be stabilized over the tetrahedral form. Verification of this hypothesis would require a dynamical simulation at ambient temperatures with the explicit inclusion of solvent. Ab initio molecular dynamics simulations of $Pu(OH)_4$ in bulk liquid water are currently in progress. Our preliminary results indicate that the planar structure is indeed stabilized in the presence of water; we are now extending the length of the simulation to ensure convergence of all ground state observables.

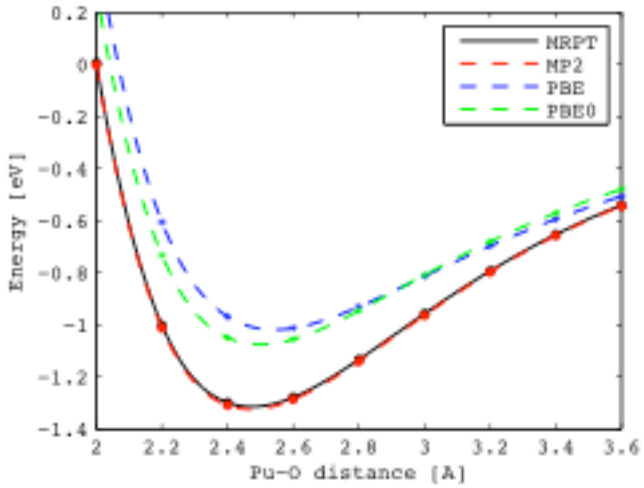

Figure D3: Planar $Pu(OH)_4 – H_2O$ potential energy. The water molecule is oriented with the O atom pointed towards Pu, with the water approaching along the normal to the $Pu(OH)_4$ plane.

In order to obtain meaningful spectroscopic data to examine the structure of aqueous Pu hydrolysis species, aqueous concentrations high enough for detection are required. A selection of resins for Pu(IV)-hydroxide XAS measurements was investigated and summarized in the Appendix.

Program Element E: Direct and Indirect Microbial Interactions with Pu and Colloids

(Duane Moser, Lead; Jen Fisher)

Microorganisms are associated with a variety of radioactive materials at DOE sites (BARNHART et al., 1980; FRANCIS et al., 1980; FREDRICKSON et al., 2004), and it is becoming well-known that Pu speciation and solubility are affected by microorganisms (GILLOW et al., 2000; NEU et al., 2005; PANAK and NITSCHE, 2001). This Program Element tests the hypothesis that environmental microorganisms can impact the mobility of Pu by direct and indirect mechanisms at environmentally relevant concentrations.

> *A range of common microorganisms from DOE sites are capable of mediating Pu reduction or biosorptive removal by a combination of direct and indirect mechanisms. Microbial alteration of mineral/colloid surfaces and production of natural organic matter will impact Pu sorption/desorption. Microorganisms will mediate the dissolution of test cavity melt glass, facilitating at least the temporary release of sequestered Pu.*

Testing this hypothesis requires screening a range of dominant microbial physiotypes from DOE sties for the capacity to mediate Pu mobilization/immobilization under physiological conditions. We have designed laboratory studies to determine if microorganisms can grow with Pu as a terminal electron acceptor and to attempt to determine how Pu is localized and speciated when present together with a variety of cell types. Pu-interacting microorganisms will be incorporated into several other Program Elements (*e.g.,* A, B, and D) focused on Pu sorption/desorption on mineral surfaces and colloids. The role of microbial exudates as ligands promoting or competing with Pu binding to natural surfaces will be emphasized in the follow-on years.

The reduction of U(VI) and Tc(VII) by metal-reducing bacteria for the purpose of *in situ* stabilization (bioremediation) has been extensively examined by DOE (ANDERSON et al., 2003; LOVLEY, 2003), but

microbial research involving Pu remains comparatively understudied. Most Pu microbiology to date has been performed on a handful of laboratory strains (MACASKIE and BASNAKOVA, 1998; JOHN, 2001; RUSIN et al., 1994; FRANCIS, 2007; PANAK and NITSCHE, 2001) and at relatively high Pu concentrations (micromolar to millimolar). The general lack of knowledge concerning the diversity, biodensity, exopolymer production potential, and direct Pu-reduction capacity of microorganisms at Pu-contaminated DOE sites is a knowledge gap that needs to be filled in order to assure that DOE's long-term stewardship goals are met.

In FY10 we met our milestones in Task E1 of screening a range of dominant microbial physiotypes from the Nevada Test Site despite limited sampling opportunities for hot wells at the NTS in FY10. Three major objectives were to: identify the Pu-interactive microorganisms from the Nevada Test Site, determine if the isolated microorganisms can be grown in the lab, and initiate experiments with one of these new organisms at environmentally relevant Pu concentrations (10^{-12} – 10^{-16} M).

Task E1: Survey of Pu-Interactive Microorganisms

In addition to the direct effects of microorganisms, two indirect microbial processes (ligand production and mineral alteration) could influence Pu mobility at the NTS. It is well known that natural and artificial complexants impact the solubility of Pu (*e.g.,* (KERSTING et al., 1999)). Microorganisms can produce a variety of such ligands (*e.g.*, siderophores (JOHN, 2001) and extracellular polymeric substances (EPS) (HARPER et al., 2008)) or may themselves be viewed as colloids because they fall within the appropriate size range (*e.g.*, 1 nm to 1 mm (LAWRENCE, 1996). They may also mediate the production of organic ligands such as humic and fulvic acids *via* their role in the decomposition of biological material. It is also well established that Pu interacts with mineral colloids (*e.g.*, clays, Fe-oxides) (KERSTING et al., 1999, NOVIKOV et al., 2006). Nevertheless, the question of how microbial weathering of these materials impacts actinide sorption remains unaddressed.

In FY10 we conducted both fieldwork and laboratory experiments that will provide the starting material and baseline data for experiments to be conducted in FY11 and subsequent years. UGTA field sampling (2 wells: ER-EC-11 (clean) and ER-20-7 (contaminated)) was limited to the last quarter of FY10. ER-20-7 is a radioactive far-field well, ~900 m deep, located on the Pahute Mesa (DOE, 2010) downgradient from the Benham underground nuclear test. Tritium concentrations in the tuff layers of the saturated zone were $>10^7$ pCi/L and low levels of $^{239/240}$Pu were detected as well. The high activity and presence of Pu at this site make it an ideal location for finding relevant microbial communities. Microbial communities from these samples are in the process of being characterized. Due to the late access of field sampling, the focus of our FY10 effort was on archived samples taken in FY09. Laboratory experiments included enrichment for a variety of microbial physiotypes from NTS and initial screening of NTS organisms for Pu interaction. We also began the groundwork for examining the role of microbial exudates as ligands that could promote or competing with Pu binding to natural surfaces.

Archived fluids previously collected from the NTS (water from Tunnel U12N.10) were used to obtain microbial enrichments capable of manganese oxide and iron oxide respiration (Figure E1) and aerobic EPS-producing cultures. Work is underway to obtain and characterize pure isolates from these enrichments for use in future experiments. This work will continue in FY11. Similar efforts will be applied to water collected from ER-20-7 once the sampling occurs.

The major focus of our work this year has been to assess the capacity of characterized microorganisms (e.g. *Shewanella* str. MR-1 and *Shewanella* str. CN-32) already used by DOE for radionuclide microbiology work to survive under conditions compatible with future sorption experiments in Program Element A. The goals were to 1) develop methods to assess the viability of stationary phase cells, 2) correlate these methods such that a proxy method could be used to accurately determine viable cell numbers in an experiment, and 3) use these data to select appropriate strains for future experiments.

Figure E1. The tube on the left shows (sterile) iron(III) oxide (brown) medium, while the tube on the right contains organisms that have reduced the amorphous iron oxide to magnetite (black).

Methods used thus far include spectroscopy (OD_{600}), serial dilution/plating, and flow cytometry (viable vs. total cells; Figure E2). OD_{600} readings are by far the quickest and simplest method, but only provide qualitative data. This method is best when used with a pure culture that has been calibrated with plate counts and/or flow cytometry if quantitative data is desired. Flow cytometry provides quantitative data on a culture, including the number of cells per mL and the fraction of those cells that are viable using two different cell staining methods. For fresh cultures such as those shown in Figure E3, total cells and viable cells are statistically equivalent, and the log of the cell numbers per mL is well-correlated with the OD_{600}. However, when dealing with radioactive samples, serial dilution and plating may be the only method available due to potential contamination of instruments used in the other two methods. We use these methods to estimate or quantify the number of cells per mL or per total experiment in order to calculate the dry weight of cell material. The dry weight is used to calculate K_d values for sorption.

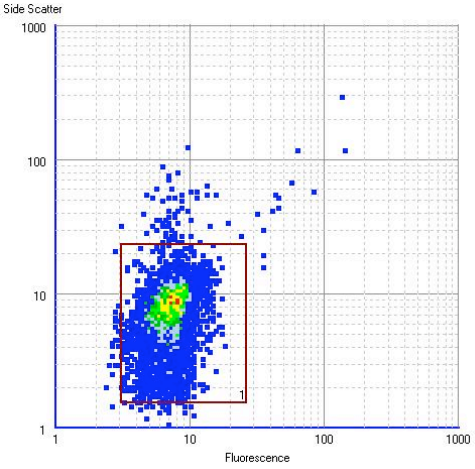

Figure E2. Flow cytometry data for a culture of *Shewanella* CN-32. Cells are stained with a nucleic acid (DNA/RNA)-binding dye that fluoresces as cells pass through a laser beam in a single-file stream.

Four *Shewanella* strains were grown to stationary phase, rinsed with a biological buffer (PIPES, 0.01 M) to adjust the cells to the desired ionic strength, and re-suspended in a nutrient-free solution with an ionic strength of 0.01 M and a pH of 3, 5, 7, or 9. Cell densities were monitored by spectroscopy (OD_{600}) and flow cytometry; viability was confirmed by plating cells on agar medium. Based on the viability of str. CN-32 across the pH range, it was selected for use in sorption experiments.

An initial sorption experiment was conducted (at I=0.01M, pH=7) to establish a baseline for sorption of Pu(IV) to cells of *Shewanella* CN-32 grown in liquid culture, *Shewanella* CN-32 grown on plates (to increase EPS), *Shewanella* CN-32 DM2 (EPS^- mutant; M. Leonardo, unpublished data), U12n.10-R (an EPS-producing microorganism isolated from the NTS, this work), and cell debris from lysed cells of *Shewanella* CN-32. The Kd values for the different treatments ranged threefold, from ~2-6 x 10^3 g/mL (Figure D4A). At the concentrations of Pu(IV) (~$7x10^{-10}$ M) and cell material used (~10^9 cells/mL), the percent Pu(IV) sorbed was similar across the various treatments. A high percentage (70-90%; Figure D4B) of the Pu present sorbed to cells almost instantly (in 0.25 h) suggesting that biological material in the environment would sorb Pu, even under

transport conditions with low residence times/high flow rates. Pu remained sorbed after 24 hours as well. Lysed cells of CN-32 had the highest K_d and sorbed the greatest percentage of Pu, possibly due to the increased surface area made available by compromised cell membranes. This observation is also important because it shows that cells do not need to take up Pu into the periplasm or cytoplasm to produce a biosorptive effect. Also notable were the higher K_d values for treatments with higher EPS contents, suggesting that Pu may sorb primarily to EPS as has been shown for other actinides. These results will be presented at the fall AGU meeting in San Francisco . The abstract is included in the Appendix.

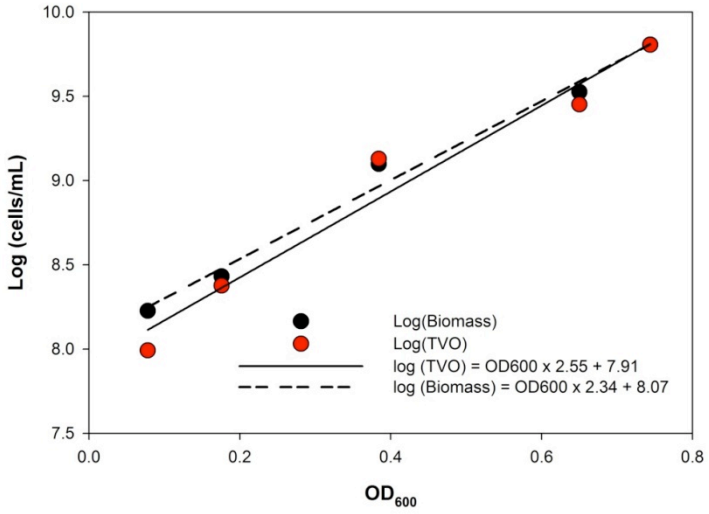

Figure E3. Correlation between optical density of *Shewanella* CN-32 at 600 nm and the total (black) or viable (red) cells per mL present in the solution.

To achieve the objective of this task, we established four types of microbial enrichment cultures: manganese oxide reducing bacteria, iron oxide reducing bacteria, and two types of aerobic heterotrophs (½ R2A and ½ LB+FLA). Although we have not purified and characterized these isolates yet, we demonstrated that one EPS-producing isolate had a relatively high Kd for Pu sorption and that sorption of Pu occurred in both whole and lysed cells.

The overall objective of this task is to determine the relative importance of secondary microbial effects on Pu sorption to minerals and mineral colloids. In support of this task, we have developed active cultures of iron and manganese oxide reducing organisms that can be used to alter the goethite synthesized for Element A. EPS from different organisms (NTS isolates, Shewanella spp.) has yet to be characterized; but methods for purification have been researched and initial testing of these methods has been initiated.

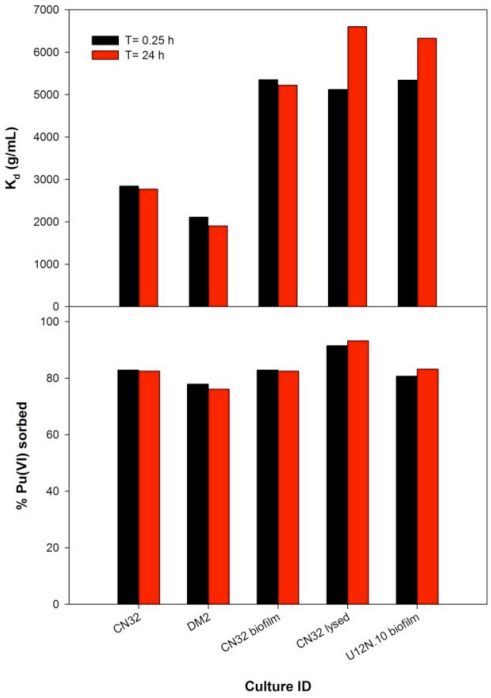

Figure E4. A) K_d values and B) % Pu sorbed by microbial cultures. Sorption occurred rapidly and changed little over a 24-hour period.

4.a.ii Scientific Highlights

Successful measurement of Pu at ultra-trace levels using CAMS. Plutonium-goethite sorption experiments were performed to aqueous concentrations below 5×10^{-17} M, equivalent to the detection of 3×10^{6} atoms in a 100 mL sample. This CAMS capability will allow us to readily perform laboratory experiments that cover the range of environmental Pu concentrations of interest.

Demonstrated Pu detection using NanoSIMS at concentrations as low as 0.7 ppm Pu on goethite. This is well below the concentrations at which Pu nano-colloids were observed by TEM and surpassed expectations outline in the SFA proposal.

Identified Pu nano-colloids lattice distortion when sorbed to goethite resulting in the formation of a bcc, Pu_4O_7 structure. This distortion results from an epitaxial growth of colloidal plutonium on goethite and provides new insight into the molecular scale behavior of Pu and how that may facilitate its transport in the subsurface.

Imaged nanometer-scale Pu distribution on Hanford sediments located 60 feet beneath a disposal crib using the NanoSIMS. Additional work to identity the mineral association of Pu will greatly help us understand how Pu moves in the subsurface.

Applied first-principles, *Ab initio,* modeling to show that in an aqueous environment the planar form of $Pu(OH)_4$ isomer can potentially be stabilized over the tetrahedral form.

4.a.iii Summary of Publications

Publications were highlighted in each Program Element where appropriate. To summarize, we presented one poster at Pu Futures in September, and 2 abstracts were submitted to fall AGU. One manuscript was recently submitted to ES&T for work in Program Element C. One master's thesis was completed on work in Program Element B. Publications are listed below and can be found in the Appendix:

Powell, B.A.**,** Zurong Dai, Mavrik Zavarin, Pihong Zhao, Annie B. Kersting. *Stabilization of Plutonium Nano-Colloids by Epitaxial Distortion on Mineral Surfaces*, Submitted to ES&T.

Zimmerman, T. N. "Plutonium humic acid stability constant determination and subsequent studies examining sorption in the ternary Pu(IV)-humic acid-gibbsite system" M.S. Thesis, Clemson University, 2010.

B.A. Powell, Z. Dai*, M. Zavarin*, A.B. Kersting*. *Structure of Plutonium Colloid When Associated with Different Minerals.* Invited: Asian Pacific Symposium on Radiochemistry *Nov. 29-Dec. 4, Napa CA, 2009*

Annie B. Kersting[1], Mavrik Zavarin[1], Zurong Dai[1], Andy Felmy[2], Ruth A. Kips[1], Duane Moser[3], Brian A. Powell[4], Ruth Tinnacher , Pihong Zhao[1] *Subsurface Transport of Pu on Nanominerals: Teasing out Biogeochemical Controls in Field Environme*nt Invited:*: Goldschmidt, June 13-18, Knoxville TN, 2010*

Zhao, P. et al. *Pu Sorption to Goethite at Micromolar to Attomolar Concentrations*. Abstract Pu Futures-The Science, Sept 19-23, 2010, Keystone CO

Zhao, P. et al. *Isotherm of Pu/Goethite System: Linearity and Sorbent Surface Characterization*. Abstract submitted to AGU, San Francisco, Dec. 15-19, 2010

Snow, M. et al. *Neptunium Sorption to Geothite*. LLNL summer student poster session, Aug. 8, 2010 LLNL-POST-448451.

Fisher, J. et al. *Microbially Produced Organic Matter and Its Role in Facilitating Pu Transport in the Deep Vadose Zone*. Abstract submitted to AGU, San Francisco, Dec. 15-19, 2010

Huang, P. & Schwegler, E. *Structure and Dynamics of Liquid Water on Surfaces From ab initio Molecular Dynamics: Graphene/Water and Alumnina/Water*. ACS, San Francisco, March 2010.

4.b Future Scientific Goals

Program Element A: We will initiate a series of Pu sorption experiments on montmorillonite clay that parallel the experiments with goethite and build upon earlier high concentration studies (manuscripts in preparation). We will begin quantifying desorption rates at femtomolar Pu concentrations using goethite and/or montmorillonite in a flow-cell apparatus.

Program Element B: We will study Pu-EPS and Pu-fulvic acid aqueous complexation and quantify complexation constants. We will examine the effect of ternary systems on sorption/desorption kinetics.

Program Element C: We continue our investigation of Pu epitaxial growth on mineral surfaces. The focus will initially be on Pu polymerization on the aluminum analog of goethite (diaspore, a-AlOOH). Intercalation of Pu in montmorillonite will be investigated as a potential irreversible sorption mechanism. We will continue to evaluate Hanford and Tomsk sediments using NanoSIMS. We will evaluate the structure of Pu on the surface of another series of mineral building from our initial work on goethite.

Program Element D. *Ab initio* modeling effort will focus on simulation of monomeric Pu on simple mineral surfaces and in the presence of water. In addition, sampling and characterization of long-term melt-glass alteration experiments begun in FY10 will examine Pu association with glass alteration phases.

Program Element E: We will study microbially enhanced glass dissolution and its potential effect on Pu mobilization. Ternary sorption experiments using microbes and their exudates isolated from the Nevada Test Site contaminated wells will be initiated.

4.c New Scientific Results

See section 4.a.ii

4.d. Collaborative Research Activities

We have two sub-contracts to collaborate with two external research groups. The first is with Brian Powell at Clemson University, SC to work on Program Element B. Details of the work are discussed in section 4.a.i, Program Element B. The second sub-contract is with Duane Moser from the Desert Research Institute, NV to work on Program Element E. Details of the work are discussed in section 4.a.i Program Element E.

We initiated two unfunded research collaborations to investigate contaminated samples from Hanford with Andy Felmy (PNNL) and Tomsk, Russia with Stepan Kalmykov (Moscow State Universtity. Details and results from these collaborations can be found in Section 4.a.i, Program Element C, Task C2.

5. Staffing and Budget Summary

5.a Funding Allocation by Program Element

5.a.i Present Funding

Our SFA is currently funded at 1.2M/yr for 5 years beginning Oct. 2009. We have approximately 200K carryover that will be used to fund our new LLNL postdoc in FY11.

Program Element	Costs (K)	LLNL Researcher	Effort	Cost (K)*
Program Element A	388	Annie Kersting	15%	91
Program Element B (Subcontract Clemson Univ.)	110	Mavrik Zavarin	60%	246
Program Element C	179	Pihong Zhao	60%	168
Program Element D	215	Patrick Huang	50%	204
Program Element E (Subcontract DRI)	140	Zurong Dai	20%	72
		Scott Tumey	20%	55
		Ruth Kips	50%	62
		Ruth Tinnacher	25%	12
Total	1,032K	LLNL effort		910K

*Effort costs for LLNL staff do not include supplies, analytical costs or travel.

5.b Funding for External Collaborators

External collaborators are: Brian Powell at Clemson University, SC. He is funded by a sub-contract for $110K/year for work in Program Element B. He completed his milestones. Our second collaborator is Duane Moser from Desert Research Institute, NV. He is funded at $140K/yr for work in Program Element E. He completed his milestones. Both these efforts will continue in FY11 at approximately the same level of funding.

5.c Personnel Actions

Because this is a new SFA, all staff were brought onto the project this year. This includes 8 staff scientists, 4 postdocs and 1 student at LLNL. Collaborations from 2 other institutions were also initiated that include 2 lead scientists, 1 postdoc and 3 graduate students. As part of our efforts to encourage young investigators and hire new staff, we converted one LLNL postdoc to a flex-term staff scientist in October, 2009. His focus is on applying advanced computational modeling techniques to environmental radiochemistry problems and specifically worked on Program Element D with overlap with Program Element A. We recently hired one new postdoc in August, 2010 and he will focus on Program Element A. We currently have 4 postdocs working on this program in Program Elements A, B, C and D. We had one student from Washington State working on Program Element A. No personnel have been released from this project since its inception at the beginning of FY10.

5.d National Laboratory Investments

The Seaborg Institute covers all of the administrative costs to execute this program, approximately 15% of an Administrator's time. In addition, the SEM operational cost is also covered under the Institute's operating budget. Annie Kersting, Director of the Seaborg Institute oversees a summer student program that paid for the cost of one summer student working on this program in FY10.

As an institution, LLNL subsidizes the cost of all the postdoc by 25%.

Several pieces of equipment were purchased in FY10 and FY11 by other programs that will directly benefit BER. They are: low energy gamma counter (Canberra), BET (Quantachrome Quadrasorb with low surface area Kr option), XRD and Deltech furnace (glass synthesis applications). All equipment is available for this program. LLNL has committed to refurbishment of Building 151 (the primary location of SFA facilities). This will involve laboratory refurbishment and modernization, as well as the purchase of new analytical instruments. As part of this renovation, a new low-level lab will be constructed for use by this SFA.

5.e Capital Equipment

Capital equipment purchases are not planned for FY11.

6. References

Anderson R. T., Vrionis H. A., Ortiz-Bernad I., Resch C. T., Long P. E., Dayvault R., Karp K., MarutzkyS., Metzler D. R., Peacock A., White D. C., Lowe M., and Lovley D. R. (2003) Stimulating the insitu activity of *Geobacter* species to remove uranium from the groundwater of a uranium contaminated aquifer. *Appl. Environ. Microbiol.* **69**(10), 5884-5891.

Barnhart B.J., Campbell E.W., Martinez E., Caldwell, and Hallet. (1980) Potential microbial impact on transuranic wastes under conditions expected in the Waste Isolation Pilot Plant (WIPP). In Annual Report. Los Alamos National Laboratory.

Davis, J. A., Gloor, R. Adsorption of dissolved organics in lake water by aluminum oxide. Effect of molecular weight. *Environ. Sci. Technol*., 15, 1223-1229, 1981.

Demirkanli D.I, Molz F.J., Kaplan D.I., and Fjeld R.A. (2008) A fully transient model for long-term plutonium transport in the Savannah River Site vadose zone: Root water uptake. *Vadose Zone Journal* **7**(3), 1099-1109.

Dzombak D.A. and Morel F.M.M. (1990) *Surface complexation modeling: hydrous ferric oxide*. Wiley.

Eng P.J. et al., (2000) *Science* 288, 1029

Francis A. J., Dobbs S., and Nine B. J. (1980) Microbial Activity of Trench Leachates from Shallow- Land, Low-Level Radioactive-Waste Disposal Sites. *Applied and Environmental Microbiology* **40**(1), 108-113.

Francis A. J. (2007) Microbial mobilization and immobilization of plutonium. *Journal of Alloys andCompounds* **444**, 500-505.

Fredrickson J. K., Zachara J. M., Balkwill D. L., Kennedy D., Li S. M. W., Kostandarithes H. M., Daly M. J., Romine M. F., and Brockman F. J. (2004) Geomicrobiology of high-level nuclear waste contaminated vadose sediments at the Hanford Site, Washington State. *Applied and Environmental Microbiology* **70**(7), 4230-4241.

Gillow J. B., Dunn M., Francis A. J., Lucero D. A., and Papenguth H. W. (2000) The potential of subterranean microbes in facilitating actinide migration at the Grimsel Test Site and Waste Isolation Pilot Plant. *Radiochimica Acta* **88**(9-11), 769-774.

Glynn P. D. (2003) Modeling Np and Pu transport with a surface complexation model and spatially variant sorption capacities: Implications for reactive transport modeling and performance assessments of nuclear waste disposal sites. Computers & Geosciences **29**(3), 331-349.

Harper R. M., Kantar C., and Honeyman B. D. (2008) Binding of Pu(IV) to galacturonic acid andextracellular polymeric substances (EPS) from *Shewanella Putrefaciens*, *Chlostridium* sp. and*Pseudomonas fluorescens*. *Radiochimica Acta* **96**, 753-762.

John S. G., Christy E. Ruggiero, Larry E. Hersman, Chang-Shung Tung, and Mary P. Neu. (2001) Siderophore mediated plutonium accumulation by Microbacterium flavescens (JG-9). *Environmental Science & Technology* **35**, 2942-2948.

Kaplan, D.I., Powell B.A., Demirkanli D.I., Fjeld R.A., Molz F.J., Serkiz S.M., and Coates J.T. (2004) Influence of oxidation states on plutonium mobility during long-term transport through an unsaturated subsurface environment. *Environmental Science & Technology*. **38**(19), 5053-5058.

Kaplan, D.I.. Powell B.A., Gumapas L., Coates J.T., Fjeld R. A., and Diprete D.Pl (2006) Influence of pH on plutonium desorption/solubilization from sediment. *Environmental Science & Technology **40**(19), 5937-5942.*

Kersting A. B., Efurd D. W., Finnegan D. L., Rokop D. J., Smith D. K., and Thompson J. L. (1999) Migration of plutonium in ground water at the Nevada Test Site. *Nature* **397**(6714), 56-59.

Lawrence J. R. H. M. J. (1996) Transport of bacteria through geologic media (review). *Can. J. Microbiol.* **42**, 410 - 422.

Lovley D. R. (2003) Cleaning up with genomics: applying molecular biology to bioremediation. *Nat Rev Microbiol* **1**(1), 35-44.

Macaskie L. E. and Basnakova G. (1998) Microbially enhanced chemisorption of heavy metals: A method for the bioremediation of solutions containing long lived isotopes of neptunium and plutonium. *Environmental Science & Technology* **32**(1), 184-187.

Neck V., Altmajer M., Seibert A., Yun J.I., arquardt C.M., and Fanghanel T. (2007) Solubility and redox reactions of Pu(IV) hydrous oxide: Evidence for the formation of PuO2+X (s, hyd.) *Radiochimica Acta* 95(4), 193-207.

Neu M. P., Icopini G. A., and Boukhalfa H. (2005) Plutonium speciation affected by environmental bacteria. *Radiochimica Acta* **93**(11), 705-714.

Novikov, A.P., Kalmykov, S.N., Utsunomiya, S., Ewing, R.C., Horreard, F., Merkulov, A., Clark, S.B., Tkachev, V.V., Myasoedov, B. F. Colloid transport of plutonium in the far-field of the Mayak Production Association, Russia, *Science* 314, 638 (2006).

Panak P. J. and Nitsche H. (2001) Interaction of aerobic soil bacteria with plutonium(VI). *Radiochimica Acta* **89**(8), 499-504.

Pickett D.A. (2005) Approach to assessing the potential effects of colloidal radionuclide transport on nuclear waste repository performance. *Nuclear Science and Engineering* **151**(1), 114-120.

Powell, B.A., Fjeld, R.A., Kaplan, D.I., Coates, J.T., Serkiz, S. M. $Pu(V)0_2^+$ adsorption and reduction by synthetic hematite and goethite," *Environmental Science & Technology* 39, 2107 (2005).

Powell B. A., Kersting A. B., Zavarin M., and Zhao P. "Development of a Composite Non-Electrostatic Surface Complexation Model Describing Plutonium Sorption to Aluminosilicates" Lawrence Livermore National Laboratory, LLNL-TR-408276, 2008.

Rusin P. A., Quintana L., Brainard J. R., Strietelmeier B. A., Tait C. D., Ekberg S. A., Palmer P. D.,Newton T. W., and Clark D. L. (1994) Solubilization of Plutonium Hydrous Oxide by Iron-Reducing Bacteria. *Environmental Science & Technology* **28**(9), 1686-1690.

Soderholm, L., Almond P.M., Skanthakumar S., Wilson, R.R., and Burns, P.C. (2008) The structure of the plutonium oxide nanocluster *Angewandte Chemie-International Edition* **47**(2), 298-302.

Tien N.C. and Jen C.P. (2007) Analytical modeling for colloid-facilitated transport of N-member radionuclide chains in the fractured rock. *Nuclear Science and Techniques* **18**(6), 336-343.

U.S. Dept. Energy, (2007) Basic research needs for geosciences; facilitating 21st centrury energy systems. Report from the workshop Feb. 21-23, 2007, pp. 186

Van Loon LR, Granacher S, Harduf H. Equilibrium dialysis—ligand exchange: A novel method for determining conditional stability constants of radionuclide—humic acid complexes. Analytica Chimica Acta 1992; 268(2):235-46.

Zimmerman, T. N. "Plutonium humic acid stability constant determination and subsequent studies examining sorption in the ternary Pu(IV)-humic acid-gibbsite system" M.S. Thesis, Clemson University, 2010.

Appendix

Task A1: Quantifying Pu Sorption Behavior on Geothite Over a Ten Order of Concentration Range

Kinetic analysis of Pu(V) and Pu(IV) Sorption to Goethite

Kinetic data provide additional insight into Pu sorption behavior. In the absence of goethite, 5×10^{-8} mol/L Pu(V) is stable in solution over the two week experiment time period (Figure A4a). In contrast, Pu(IV) at that same concentration decreases by an order of magnitude. The instability of Pu(IV) can be attributed to homogeneous nucleation of PuO_2(am) whose solubility is reported to be on the order of 10^{-9} M. At lower concentrations, aqueous Pu(IV) and Pu(V) solutions were both found to be stable.

In the presence of goethite (0.1 g/L), aqueous Pu concentrations decrease rapidly in all cases (Figure A5b, A5c). Sorption kinetic data can be categorized into three distinct regimes. At the highest initial Pu concentrations ($>10^{-5}$ M), equilibrium is not reached for either Pu(V) or Pu(IV) over the two week experimental time period. The rates of Pu(V) and Pu(IV) sorption are equivalent, most likely controlled by a combination of homogeneous and heterogeneous PuO_2(am) nucleation rates. Pu(V) reduction to Pu(IV), catalyzed by the goethite surface or via disproportionation to Pu(IV) and Pu(VI) in the aqueous phase, does not appear to be rate limiting. Between 10^{-5} and 10^{-7} M Pu, the rates of Pu(IV) sorption are markedly faster than Pu(V). A combination of homogeneous and surface nucleation of Pu(IV) results in rapid Pu sorption. For Pu(V) at these concentrations, surface catalyzed Pu(V) reduction controls the rate of apparent Pu sorption. The reduction was confirmed by TEM analysis of the Pu-goethite solids. At concentrations $<10^{-7}$ M, sorption appears to reach equilibrium within 7 days for both Pu(IV) and Pu(V). Furthermore, the aqueous concentration at equilibrium does not appear to be a function of the initial oxidation state of Pu. The surface catalyzed reduction of Pu(V) to Pu(IV) occurs on the scale of days, consistent with Pu(V) sorption rates previously measured on hematite (POWELL et al., 2005).

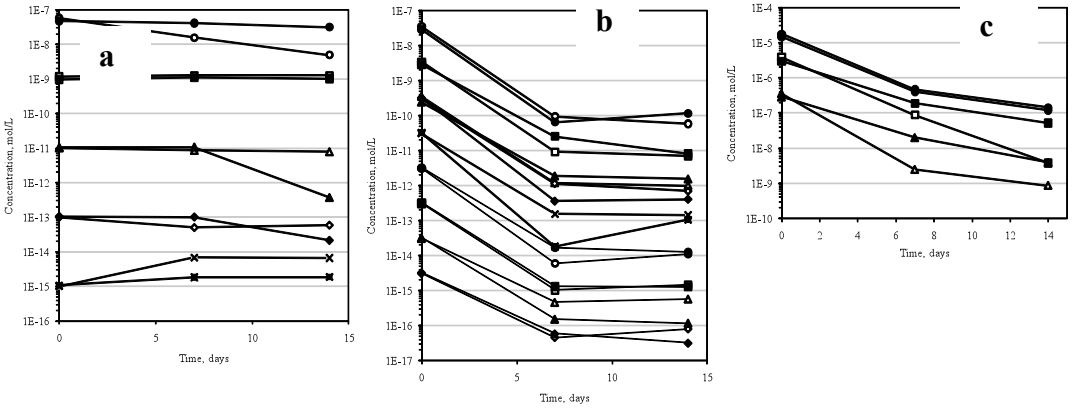

Figure A5. Aqueous Pu concentration in (a) goethite-free solutions and (b,c) 0.1 g/L solutions as a function of time with Pu initially as Pu(IV) (open symbols) and Pu(V) (closed symbols).

Invited Talk: Goldschmidt, June 13-18, Knoxville TN, 2010

Subsurface Transport of Pu on Nanominerals: Teasing out Biogeochemical Controls in Field Environments

ANNIE B. KERSTING[1], MAVRIK ZAVARIN[1], ZURONG DAI[1], ANDY FELMY[2], RUTH A. KIPS[1], DUANE MOSER[3], BRIAN A. POWELL[4], RUTH TINNACHER , PIHONG ZHAO[1]

[1]Glenn T. Seaborg Institute, Physical & Life Sciences, Lawrence Livermore National Laboratory, Livermore, CA 94550. Kersting1@LLNL.gov

[2]Pacific Northwest National Laboratory, Richland, WA 99352

[3]Desert Research Institute, Las Vegas, NV 89119

[4]Clemson University, Clemson, SC 29625

The ability of colloids (< 1 micron particules) to transport strongly sorbing radionuclides, such as plutonium (Pu), has been shown in a number of seminal field studies[1,2,3]. Despite the recognized importance of colloid-facilitated transport, little is known about the geochemical and biochemical mechanisms controlling Pu-colloid formation and association. The major challenge in predicting the mobility and transport of plutonium (Pu) is determining the dominant biogeochemical processes that control its behavior at the water-mineral interface. The reaction chemistry of Pu (*i.e.*, aqueous speciation, solubility, sorptivity, redox chemistry, and affinity for colloidal particles, both abiotic and microbially-mediated) is particularly complex.

Current research at the Nevada Test Site (NTS) has shown that the transport of Pu detected in deep groundwater with low organic carbon is associated with the inorganic colloidal fraction, specifically clays. In addition, greater than 70% of the total Pu is associated with the smallest particulates, 10-100 nm. Yet, in shallower NTS groundwater with high dissolved organic carbon, the Pu is mostly dissolved and not colloidal. In contrast, Santachi et al.[2] has shown that at Rocky Flats the Pu is associated with the microbial fraction of the surface water. At Hanford the vertical transport of Pu in the vadose zone appear to be mineralogically controlled. We will compare results from different biogeochemical environments at NTS to elucidate the dominant controls on transport of Pu in the subsurface.

[1]Kersting A.B. *et. al.* (1999) *Nature* **397**(6714), 56-59.

[2]Santschi P. *et. al.* (2002) *Env. Sci. & Tech.* **36**(17), 3711-3719.

[3]Novikov A. P et al. (2006) *Science* **314**(5799), 638-641.

Funded by Office of Science, Biological & Environmental Research. Prepared by LLNL under Contract DE-AC52-07NA27344

Pu Sorption to Goethite at Micromolar to Attomolar Concentrations

P. Zhao, M. Zavarin, S. Tumey, R. Williams, Z. Dai, R. Kips, and A.B. Kersting, G. T. Seaborg Institute, Physical & Life Sciences, Lawrence Livermore National Laboratory

Plutonium Futures —The Science 2010, Keystone, Colorado, USA, September 19-23, 2010

INTRODUCTION

A major challenge in predicting the mobility and transport of plutonium (Pu) is determining the dominant geochemical processes that control its behavior in the subsurface. Pu concentrations in groundwater samples at field sites are typically in the 10^{-12}-10^{-16} M range whereas laboratory experiments are routinely carried out at concentrations >10^{-10} M. We have previously shown that aqueous Pu(IV) underwent epitaxial growth on goethite surface as Pu_4O_7 nanocrystals. It is not known whether the same polymeric Pu is produced with Pu(V) in solution or at very low (i.e. femtomolar) concentrations. In this poster, we explore Pu morphology and sorption behavior over a concentration range that brackets field and laboratory Pu concentrations. Our long term research objective is to develop a conceptual model of Pu transport that captures the complex sorptive and morphological characteristics of Pu under relevant environmental conditions.

TEM Image of Pu associated Goethite

PuO_2 Crystal Structure

Pu_4O_7 Crystal Structure

OBJECTIVE

- **Obtain Pu-goethite sorption isotherm ranging from 10^{-7} to 10^{-17} M Pu.**
- **Compare sorption behavior of Pu(IV) to Pu(V).**
- **Examine sorption kinetics.**
- **Characterize Pu association with goethite surface.**

Model Prediction and
Detection Ranges of Various Analytical Technologies

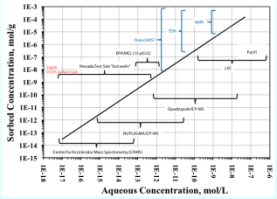

ABSTRACT

Batch sorption experiments were performed to obtain isotherms for Pu(aq, IV) and Pu(aq, V) on goethite in pH8 buffer over a wide Pu concentration range (10^{-17} to 10^{-7} M). The Pu(aq, IV) and Pu(aq, V) isotherms were very similar (surface catalyzed Pu(V) reduction to Pu(IV)) and linearity extended from 10^{-17} to 10^{-10} M Pu. Nonlinearity and slow "sorption" above 10^{-10} M Pu was due to intrinsic Pu(IV) nanocolloid formation. HRTEM identified distinctly different nanocolloids morphologies in Pu(aq, IV) and Pu(aq, V) high concentration (~10^{-7} M) samples, suggesting that the primary nucleation mechanisms were bulk (homogeneous) and surface (heterogeneous) nucleation for Pu(IV) and Pu(V), respectively. At intermediation concentrations (10^{-10} to 10^{-7} M), surface nucleation dominated for both Pu oxidation states. At lower concentrations (<10^{-10} M) HRTEM could not detect nanocolloids on the goethite surface. However, nanoSIMS showed strong correlation between Pu and goethite and uniform Pu distribution on the mineral surface at the nanoSIMS resolution for both Pu oxidation states, suggesting a possible transition to monomeric Pu distribution on the goethite surface.

METHODS

1. Batch Sorption Experiments

5mM NaCl + 0.7mM NaHCO3, pH8
0.1g/L Goethite
7 and 15 days sampling

Oxidation States	Pu Isotope Mass Percentage	Initial total Pu concentration (M)	Aqueous Pu conc (M)
Pu (IV)/ Pu(V)	~ 80% ^{239}Pu , 20% ^{240}Pu	$3x10^{-13}$ M to $3x10^{-10}$ M	$1x10^{-17}$ to $1x10^{-12}$
Pu (IV)/ Pu(V)	~ 100% ^{242}Pu	$3x10^{-10}$ to $2x10^{-5}$ M	$1x10^{-12}$ to $5x10^{-7}$

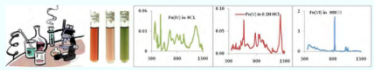

2. Aqueous Solution Analyses

Accelerator mass spectrometry, NuPlasma HR MC-ICP-MS, Quadrupole ICP-MS, and Liquid Scintillation Counting

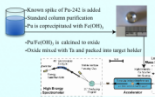

Accelerator Mass Spectrometry Analysis Scheme

2. Solid Phase Characterization

High Resolution Transmission Electron Microscopy (HRTEM)
Nano-Secondary Ion Mass Spectrometry (NanoSIMS)

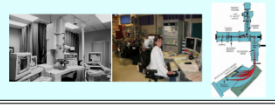

NanoSIMS Scheme

Acknowledgement

This work was funded by the Office of Science, Biological & Environmental Research, and performed under the auspices of the U.S. Department of Energy by Lawrence Livermore National Security, LLC under Contract DE-AC52-07NA27344. LLNL-POST-455811

RESULTS

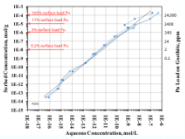

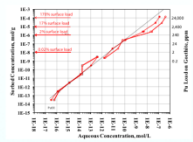

Sorption isotherms of Pu(IV) (blue circles) and Pu(V) (red circles) agree well with linear model (black line) when Pu on goethite surface is <$3x10^{-7}$ mol/g (<1% surface load). Pu(IV) and Pu(V) shows pronounced nonlinearity and time-dependence at higher concentrations due to rate-limited nanocolloid formation.

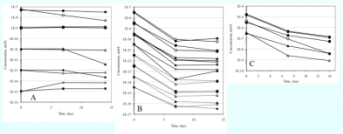

Aqueous Pu concentration as function of time with Pu initially as Pu(IV) (open symbols) and Pu(V) (closed symbols)
A. Pu in goethite-free blank solutions.
B . Pu in 0.1 g/L goethite solutions. Pu concentrations within isotherm linear range.
C. Pu in 0.1 g/L goethite solutions. Pu concentrations within isotherm non-linear range.

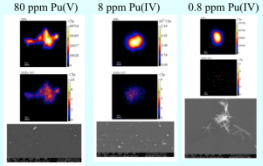

NanoSIMS images of Pu/Goethite samples show strong correlation between Fe and Pu. Images suggest even distribution of Pu on the goethite surface at resolution of the nanoSIMS. SEM images show morphology of goethite on sample holders.

RESULTS

TEM Observations and Analyses

Pu(IV)aq, ~40,000 ppm
Agglomerated nano-colloids form on goethite and carbon film, indicating bulk nucleation is the primary mechanism of crystallization at high Pu(IV) concentrations.

Pu(V), ~40,000 ppm
Nano-colloids formed with a characteristic dispersive distribution on goethite, providing evidence of heterogeneous nucleation on goethite surface. Dispersive Pu nanocrystals were predominant in Pu(V) and low conc. of Pu(IV) samples.

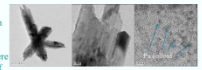

After aging for 3 months in MQW (right image), dispersive nanocrystal growth is evident. Evidence is less visible in agglomerative Pu colloid sample.

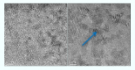

Pu(IV)aq, 800 ppm (left)
Nano-colloids were observed associated with goethite surface
Pu(V), 800 ppm (right)
Nano-colloids were not detected by TEM, suggesting diffuse (monomeric) distribution.

Crystal Structure Characterization

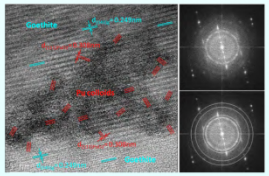

HRTEM image (left) and corresponding fast Fourier transform (FFT) (right) obtained from the sample of high concentration Pu(IV), showing agglomerative FCC PuO_2 nanocrystals randomly distributed on goethite.

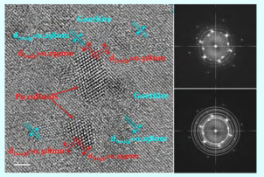

HRTEM image (left) and corresponding fast Fourier transform (FFT) (right) obtained from the sample of high concentration Pu(V), showing dispersive BCC Pu_4O_7 nanocrystals distributed on goethite in the form of epitaxial growth with {114}Pu_4O_7 || {021}goethite .

Abstract submitted to American Geophysical Union, Fall Meeting Dec. 13-17 San Francisco, CA

Isotherm of Pu/Goethite System: Linearity and Sorbent Surface Characterization

P. Zhao, M. Zavarin, S. Tumey, R. Williams, Z. Dai, R. Kips, and A.B. Kersting

Glenn T. Seaborg Institute, Physical & Life Sciences, Lawrence Livermore National Laboratory, P.O. Box 808, Livermore, CA 94550. Zhao1@llnl.gov

ABSTRACT

A major challenge in predicting the mobility and transport of plutonium (Pu) is determining the dominant geochemical processes that control its behavior in the subsurface. An improved understanding of coupled processes, from the mineral surface to the field scale, under relevant environmental conditions is essential for significant breakthroughs in Pu transport conceptual model. However, systematic studies under relevant environmental conditions are lacking.

We performed Pu(IV) and Pu(V) batch sorption isotherms in 0.7 mM $NaHCO_3$/5 mM NaCl (pH ~8) solution with goethite over a ten order of magnitude concentration range. Pu(V) is expected to reduce to Pu(IV) on the goethite surface. Aqueous Pu concentrations and surface loadings ranged from 10^{-7} to 10^{-17} M and >100% to $<10^{-7}$%, respectively. Several techniques and Pu isotopes were employed (accelerator mass spectrometry (AMS), NuPlasma HR MC-ICP-MS, quadrupole ICP-MS, and scintillation counting) to measure the concentration of aqueous Pu over the large range investigated. In addition, Transmission Electron Microscopy (TEM) and nano-secondary ion mass spectrometry (NanoSIMS) were used to investigate the morphology and distribution of Pu associated with goethite. Although the obtained isotherms for Pu(IV) and Pu(V) solutions /goethite systems are similar, distinctly different morphology of Pu nano-particles on goethite at higher concentrations were observed between the Pu(IV) and Pu(V) experiments by TEM. Furthermore, epitaxis of Pu nano-particles were found on goethite mineral surfaces.

This work was funded by Office of Science, Biological & Environmental Research Program, and performed under the auspices of the U.S. Department of Energy by Lawrence Livermore National Security, LLC under Contract DE-AC52-07NA27344. LLNL-ABS-456371.

Neptunium Sorption to Goethite

Mathew Snow, Nuclear Forensics Internship Program
Pihong Zhao, Mavrik Zavarin, and Annie Kersting, Chemical Sciences Division, PLS

Glenn T. Seaborg Institute

Introduction

Large quantities of neptunium have been released into the environment as a result of nuclear weapons programs and reactor discharge.[1] With a half life on the order of two million years, coupled with its in-growth from parent nuclide Am-241, Np-237 also represents a major contributors to the long term (~100,000+ yrs) dose of proposed geological repositories.[2]

Iron oxides, such as goethite (FeOOH), are commonly found in rocks and soils. While the degree to which these minerals (ad)sorb radionuclides has wide implications on their ability to retard actinide migration, strong sorption also has the potential to increase actinide mobility via colloid-facilitated transport.[3] Thus, an increased understanding of neptunium-goethite interactions is essential for reliable transport models, as well as possible methods for remediation and retardation.

Background

While Np(IV) and Np(VI) have been observed in highly reductive and oxic environments, respectively, Np(V) is the predominant oxidation state under typical environmental conditions.[4] Most laboratory studies have analyzed neptunium at much higher concentrations (>10^{-6} M) than are frequently observed in the environment (10^{-12} M Np observed at the Nevada Test Site), making the assumption that the processes observed in the laboratory are simply scalable to environmentally relevant concentrations.[5,6,7]

While neptunium-237 is the predominant neptunium isotope found in the environment, its relatively low specific activity makes it difficult to detect at lower concentrations (<10^{-7} M) using nuclear counting techniques. Thus, for this study a mixed approach was adopted, using Np-239 (half life of 2.345 days) for lower concentrations (10^{-18} to 10^{-15} M), a 239/237 mixture, in which Np-239 is used as a tracer, for medium range concentrations (10^{-14} to 10^{-9} M), and pure Np-237 for analysis of higher concentrations (10^{-8} to 10^{-5} M).

Objectives

- **Study the Np-goethite sorption isotherm over a wide concentration range (10^{-18} to 10^{-5} M)**
- **Analyze Kd (equilibrium constant) as a function of aqueous concentration**
- **Implement novel approach using short lived Np-239 tracers to extend the sorption isotherm to concentrations that are comparable to or lower than Np concentrations observed in the environment**

Methods

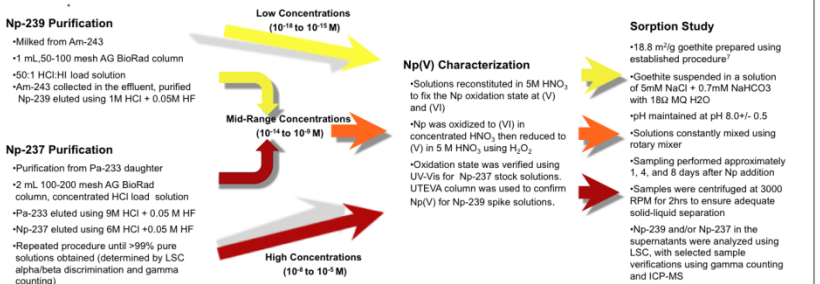

Results

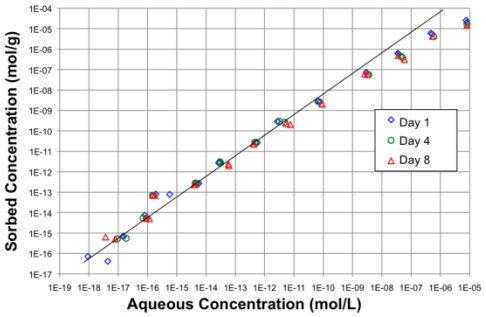

Sorption curve for Neptunium to goethite

- Sampling performed on days 1, 4, and 8 after addition of neptunium (represented in blue, green, and red respectively)
- Data follows a linear trend for neptunium concentrations between 10^{-18} to 10^{-10} M
- Begins to deviate from linearity at concentrations higher than 10^{-10} M
- Approaches surface saturation at ~10^{-5} M.

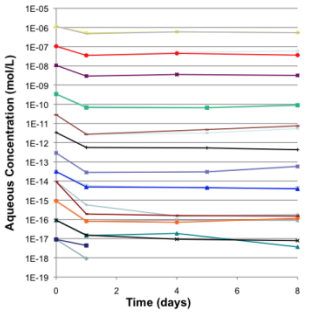

Rate Dependence of Sorption

- Equilibrium reached within first day
- Spiked blank samples showed ~15% activity loss due to sorption on container walls
- Minor increases in concentration in certain samples as a result of changes in pH

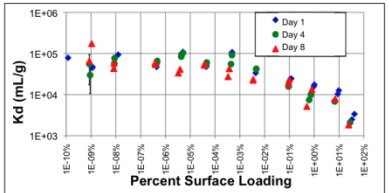

Kd as a function of percent surface loading

- Kd relatively constant from 10^{-10} to 10^{-4}% site occupation
- Decreases exponentially at concentrations greater than 10^{-4}%

Preliminary Sorption Modeling

- Concentrations <10^{-10} M aqueous Np (<10^{-4}% site occupation) support a Langmuir behavior
- Concentrations >10^{-10} M aqueous Np (>10^{-4}% site occupation) support a Freundlich behavior

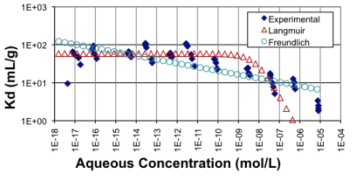

Conclusion

- **Np-goethite sorption reaches equilibrium within 1 day**
- **Kd relatively constant between 10^{-18} and 10^{-10} M (10^{-10} to 10^{-4}% surface loading) then decreases exponentially from 10^{-10} to 10^{-5} M**
- **Np-239 tracers found to extend detection limits down to ~10^{-18} M concentrations**
- **Future work includes improving modeling capabilities using 2-site Langmuir and similar approaches to elicit more information on Np-goethite sorption site affinity**

References

1-Smith, D.K., Finnegan, D.L., and Bowen, S.M., 2003. Journal of Environmental Radioactivity 67, 35-51.
2- Turner, D.R; Bertetti, F.P; Pabalan, R.T. Soil Science Society of Amercia: Madison, WI, 2002; pp211-252
3- Kersting AB., D. W. Efurd, D. L. Finnegan, D. J. Rokop, D. K. Smith, J. L. and Thompson, (1999). *Nature* 397, 56-59
4- Dozol M, Hagemann R.; *Pure Appl Chem 1993, 65:1081-1102*
5- Arai, Y., Moran, P.B., Honeyman, B.D., and Davis, J.A., 2007. Environmental Science & Technology 41, 3940-3944.
6-Nakayama, S. and Sakamoto, Y., 1991. Radiochimica Acta 52-3, 153-157.
7-Turner, D.R., Pabalan, R.T., and Bertetti, F.P., 1998. Clays and Clay Minerals 46, 256-269.
8-Schwertmann, U. and Cornell, R. M. (1991 VCH Publishers Inc., New York, NY.

his work performed under the auspices of the U.S. Department of Energy by Lawrence Livermore National Laboratory under Contract DE-AC52-07NA27344.

Post #

Task A2: Determining the Lower Limits of our Experimental Capabilities

The NanoSIMS 50 is a secondary ion mass spectrometer that produces ion images of exceptionally high spatial resolution (Fig. A1). The combination of a short working distance, normal ion beam incidence and a high brightness ion source results in a lateral resolution as high as 50-100 nm for Cs^+ primary ion bombardment, or 150-200 nm for O^- primary ions (compared to several microns for conventional SIMS instruments).

All samples described in this report were analyzed by a beam of primary O^- ions produced by a duoplasmatron. In spite of its somewhat poorer spatial resolution, O^- primary ion bombardment significantly enhances the generation of electropositive secondary ions, and hence increases the secondary Pu^+ yield by several orders of magnitude compared to Cs^+ primary ion bombardment.

In the samples investigated, the beam was rastered over the sample, while the positively-charged secondary ions produced by the sputtering process were separated and detected by a double-focusing mass analyzer. The primary ion current at the sample varied between 20 pA - 394 pA, depending on the lens used for beam collimation. A higher beam current was typically used to increase the secondary ion count rate, albeit at a lower spatial resolution due to the increased spot size. At 80 pA primary current, the beam was measured to have a spot size of 300-400 nm. The ion images that resulted from these measurements provided a 2D distribution of the secondary ion intensity as a function of beam position (the brighter the pixel, the more intense the secondary ions).

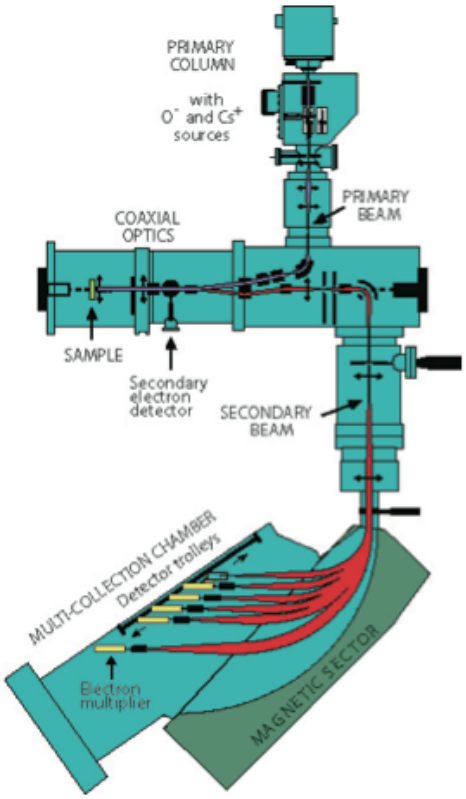

Fig. A1. Schematic of the Cameca NanoSIMS 50 secondary ion mass spectrometer.

Task B1: Screening for Enhanced Pu Mobilization by NOM

Supplementary Figures from Pu-gibbsite and Pu-gibbsite-fulvic acid sorption experiments

The figures below present supplementary data from Pu-gibbsite-fulvic acid studies. As noted in the report, sorption of Pu was monitored as a function of time but only portions of the data were presented. The data below are for the time intervals not shown in the report.

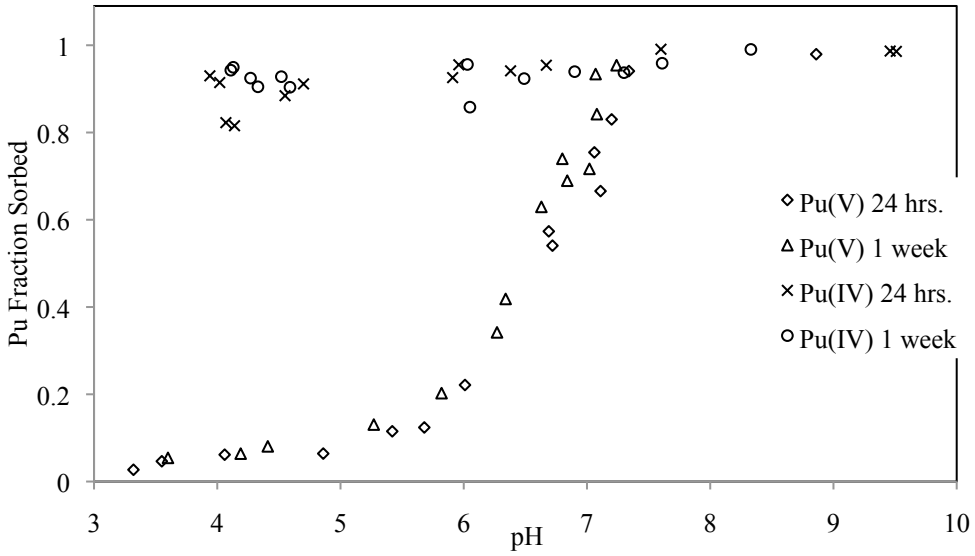

Figure B3: Pu(IV) and Pu(V) sorption to gibbsite. Concentration α-$Al(OH)_3$ = 10 g/L, ionic strength 0.1M (NaCl), $[^{238}Pu]_{total}$ = 1.3E-10 M (1000 dpm/mL), exposed to the atmosphere.

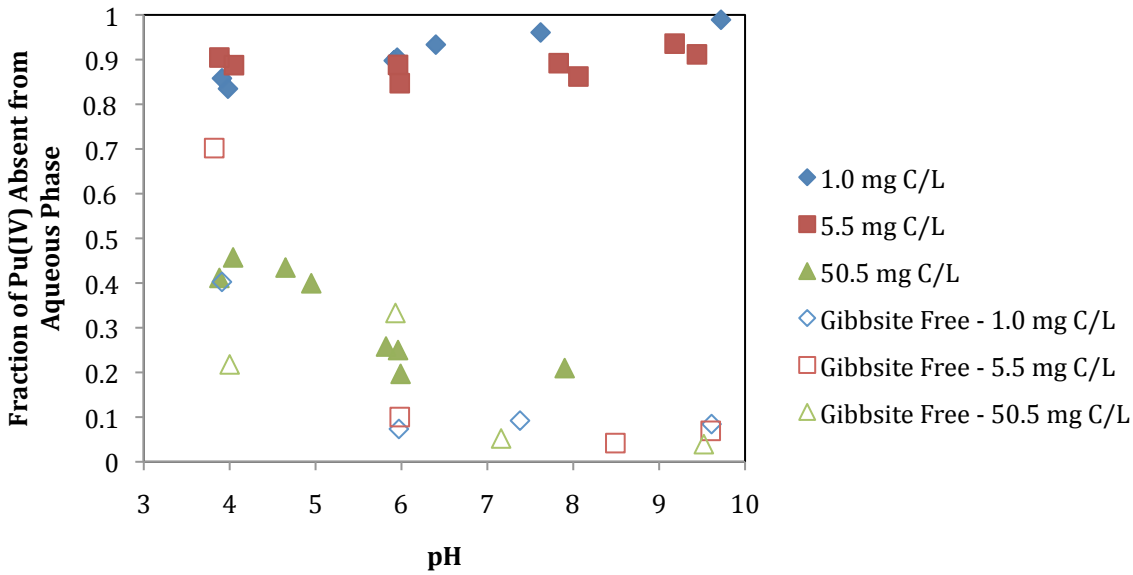

Figure 4B: Fraction of Pu(IV) absent from the aqueous phase in ternary system batch sorption experiments involving Pu(IV) at 10^{-10} M, gibbsite at 5 g/L, and fulvic acid at 1.0, 5.5, or 50.5 mg/L, by series. Open markers indicate samples that contained no gibbsite. Samples were prepared in duplicate with a 0.1 M NaCl background, and the pH was adjusted to 4, 6, 8, or 10. Samples were mixed continuously then aliquots were removed for analysis after 1, 7, and 33 days; data above is from the 1 day sampling event. Samples were passed through 30k

MWCO centrifugal filters and the Pu concentration in the filtrate was determined using liquid scintillation counting (LSC).

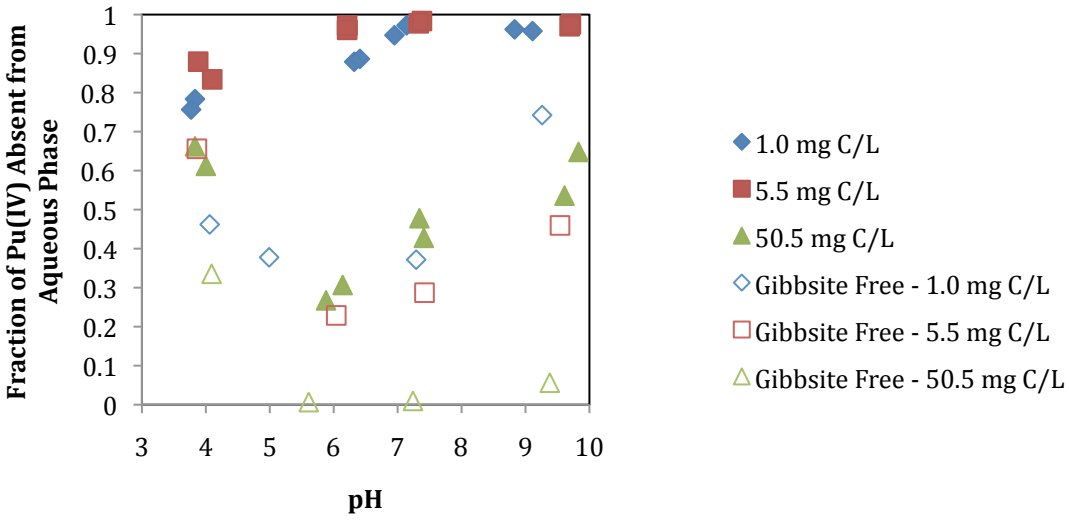

Figure B5: Fraction of Pu(IV) absent from the aqueous phase in ternary system batch sorption experiments involving Pu(IV) at 10-10 M, gibbsite at 5 g/L, and fulvic acid at 1.0, 5.5, or 50.5 mg/L, by series. Open markers indicate samples that contained no gibbsite. Samples were prepared in duplicate with a 0.1 M NaCl background, and the pH was adjusted to 4, 6, 8, or 10. Samples were mixed continuously then aliquots were removed for analysis after 1, 7, and 33 days; data above is from the 33 day sampling event. Samples were passed through 30k MWCO centrifugal filters and the Pu concentration in the filtrate was determined using liquid scintillation counting (LSC).

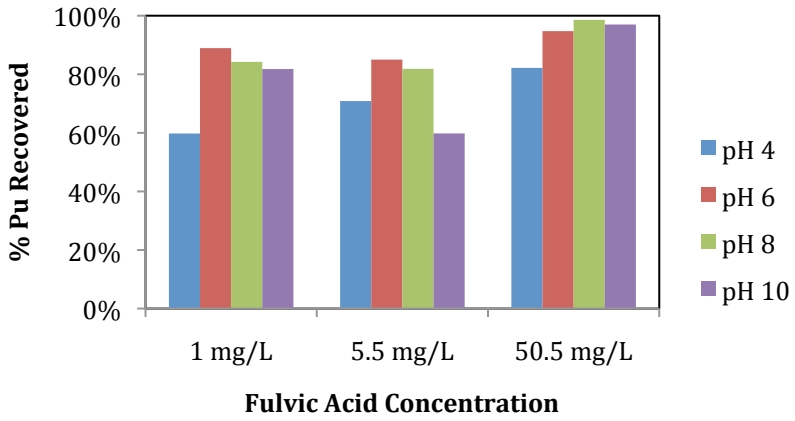

Figure B6: Total plutonium recovered after sampling events and a vial wash with 0.1 M NaOH. Data were obtained using liquid scintillation counting.

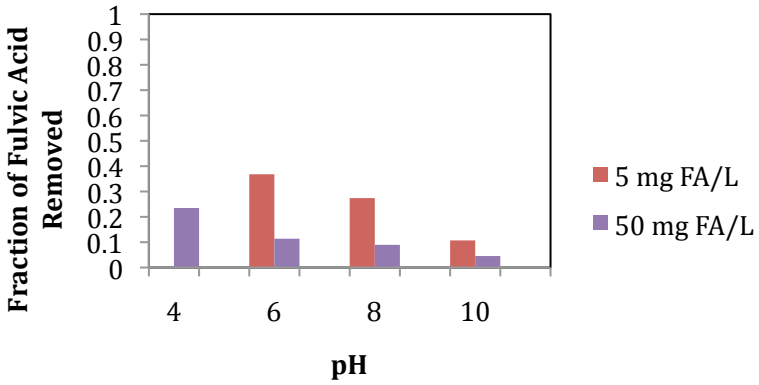

Figure B7: Fraction of fulvic acid absent from the aqueous phase. Fulvic acid may have been removed due to sorption to gibbsite, precipitation, or by the filtration step. Samples were prepared containing gibbsite at 5 g/L, and fulvic acid at 5.0 or 50.0 mg/L, by series. Samples were prepared in duplicate with a 0.1 M NaCl background, and the pH was adjusted to 4, 6, 8, or 10. Samples were mixed continuously then aliquots were removed for analysis after 1, 7, and 33 days; data above is from the 1 day sampling event. Samples were passed through 30k MWCO centrifugal filters and the fulvic acid concentration in the filtrate was determined using UV-vis spectroscopy.

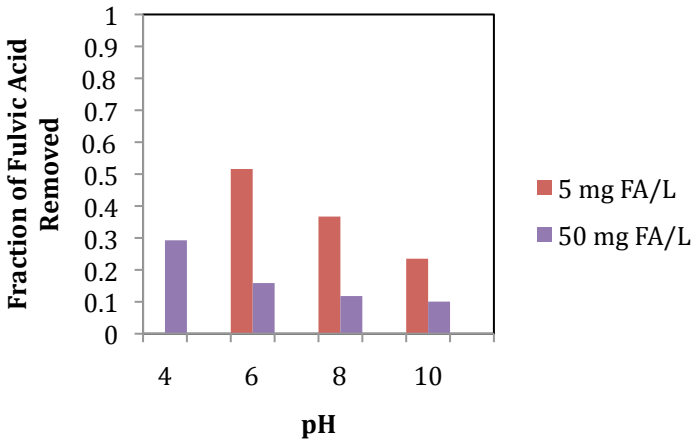

Figure B8: Fraction of fulvic acid absent from the aqueous phase. Fulvic acid may have been removed due to sorption to gibbsite, precipitation, or by the filtration step. Samples were prepared containing gibbsite at 5 g/L, and fulvic acid at 5.0 or 50.0 mg/L, by series. Samples were prepared in duplicate with a 0.1 M NaCl background, and the pH was adjusted to 4, 6, 8, or 10. Samples were mixed continuously then aliquots were removed for analysis after 1, 7, and 33 days; data above are from the 33 day sampling event. Samples were passed through 30k MWCO centrifugal filters and the fulvic acid concentration in the filtrate was determined using UV-vis spectroscopy.

Task B2: Determination of Stability Constants for Relevant Pu-NOM Complexes NOM

Supplementary Figures from Actinide-HA Complexation Experiments

Prediction of binding site concentrations on Leonardite Humic acid.

Figure B1 shows a representative potentiometric titration curve of the Leonardite humic acid used in the actinide-HA complexation experiments with model fit. The least-squared minimization program FITEQL was used to model the data. The model assumed four fixed pKa sites of 3,5,7, and 9 and the total concentration of each site was varied to fit the experimental data. As can be seen in figure 1, the model provides an excellent fit to the data. The embedded table in Figure 1contains the proton-binding site concentrations determined using FITEQL. FITEQL model output reports the concentration of species (*e.g.,* proton-binding sites) in [mol/L]. Therefore, the following equation was used to adjust the binding site concentrations to a measurable quantity, mg C (determined using TOC).

$$\left\{\frac{[HL_x]_{model}}{C_{HA,titration}(mg_C/L)}\right\} = C_{HLx}(\frac{mol}{mg_C})$$

The concentration of HLx (mol/mg C) was then scaled to the HA concentrations used in the complexation studies using the following equation, and served as input data for subsequent Pu- and Th-HA complexation models.

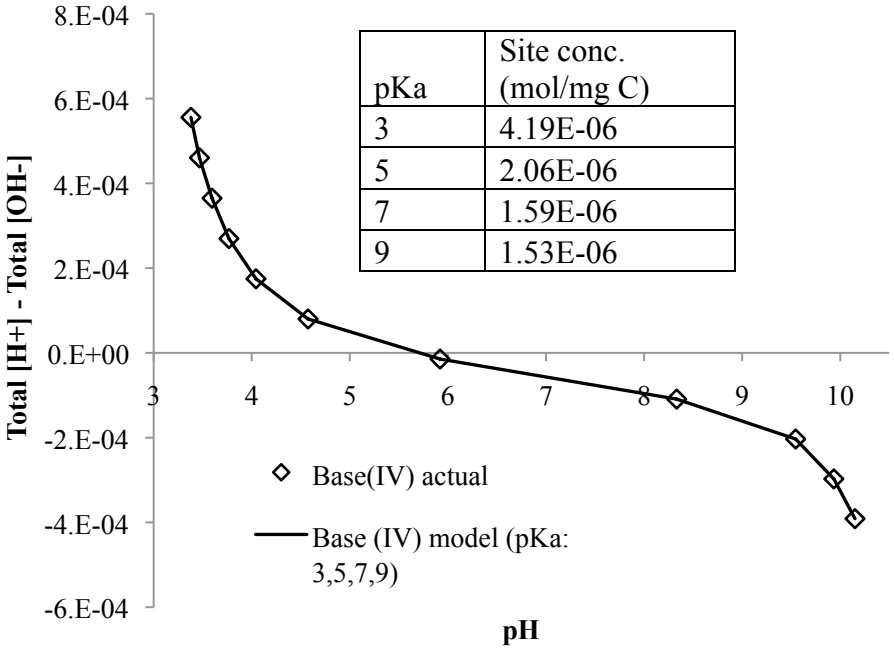

pKa	Site conc. (mol/mg C)
3	4.19E-06
5	2.06E-06
7	1.59E-06
9	1.53E-06

Figure B1: HA base (IV) titration data with model fit. Model fit generated using FITEQL assuming a discrete pKa spectrum of 3, 5, 7, and 9.

The plot below shows a linear free energy diagram of stability constants for Pu(IV)-ligand complexes and Th(IV)-ligand complexes obtained from literature values and from this work. The constants obtained in this

work agre very well with other data. This and similar plots may be used to predict the stability constants of other Pu(IV)-ligand complexes based on known interactions with Th(IV). This can greatly simplify laboratory experiments based on the relativel ease of working with Th compared with Pu.

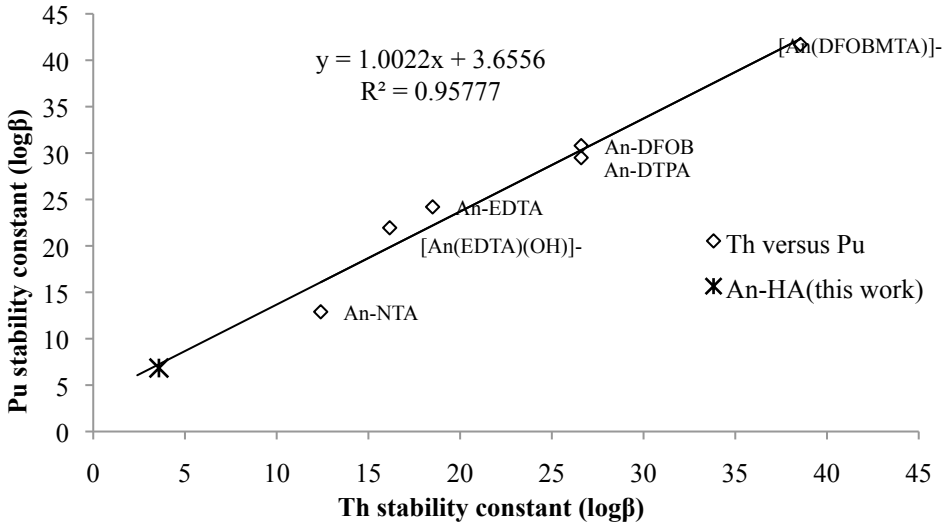

Figure B2 Plot of Th-ligand stability constants *versus* the corresponding Pu-ligand constants. The star corresponds to the stability constants determined for the 4.90E-8 M Th- and 4.35E-8 M Pu-HA datasets assuming an HL3 basis.

Abstract from Trevor Zimmerman's M.S. thesis, Clemson University, awarded spring 2010.

Plutonium has been released to the environment through a variety of intentional and unintentional mechanisms, including atmospheric testing, disposition from weapons manufacturing processes, and subsurface disposal. Therefore, a thorough understanding of the chemical, physical, and biological processes affecting plutonium transport is imperative. It has been shown that humic acid (HA) (a refractory component of natural organic matter (NOM)) can effectively solubilize plutonium (SANTSCHI *et al.*, 2002). Increased solubility may result in enhanced subsurface transport, due to the higher concentration of Pu in the aqueous phase. In contrast, the formation of ternary surface complexes may hinder actinide transport. Solution pH is likely to affect the dominance of one species over another. For these reasons, a better understanding of binary Pu-HA and Pu-mineral and ternary Pu-HA-mineral systems is essential for accurately predicting plutonium fate and transport.

The primary objective of this research was to determine the conditional stability constant for Pu-HA complexes using a hybrid ultra-filtration/equilibrium dialysis ligand exchange (EDLE) technique from pH 4 to 6.5. Ethylenediaminetetraacetic acid (EDTA) was used as a reference ligand to allow the aqueous chemistry of the Pu-HA system to be probed at increased pH, without appreciable metal hydrolysis.

The conditional stability constant for Pu(IV) complexation with Leonardite HA determined as part of this work is $\log\beta_{112} = 6.76 \pm 0.14$. This stability constant is valid over the pH range 4 – 6.5 and I = 0.1 M NaCl, for the equation shown below:

$$Pu^{4+} + HL3 + 2H_2O \leftrightarrow Pu(OH)_2L3^{+} + 3H^{+} \qquad \text{Log } \beta_{112} = 6.76 \pm 0.14$$

where HA is represented by HL3 (a binding site on the HA with a pKa value of 7).

The conditional stability constant for Th(IV) complexation with Leonardite HA was also determined. Over the pH range 4 – 6.5 the value $\log\beta_{112} = 4.63 \pm 0.04$ was calculated (I = 0.1 M NaCl) for the reaction shown below:

$$Th^{4+} + HL1 + 2H_2O \leftrightarrow Th(OH)_2L1^{+} + 3H^{+} \qquad \text{Log } \beta_{112} = 4.63 \pm 0.04$$

where HL1 represents a pKa 3 binding site on the HA.

Preliminary sorption studies using gibbsite were also conducted to evaluate the effects of Pu-HA complex formation on Pu sorption behavior. Enhanced Pu sorption to gibbsite was observed in the presence of HA. Notably, enhanced sorption was observed at low pH (pH 4) which is indicative of ligand promoted sorption. Therefore, despite observations of increased solubility of Pu in the presence of HA, the formation of ternary surface complexes may prevent enhanced subsurface transport. The data from these studies will aid in modeling the fate and transport of Pu in the environment and inform the development of conceptual models describing the influence of ternary surface complex formation on Pu sorption.

Task C2: Characterization of Pu-Colloid Interfaces on Natural Colloids

A second array of 14 ion images was collected on sample B1HK15 #2this time in peak jumping mode to include silicon (by changing the magnetic field of the analyzer). The abundance of ^{27}Al and ^{28}Si exceeded the operating limit of the detectors, therefore ^{27}AlO and ^{30}Si were measured instead (Fig. C1). Here also, the ion images of mass 239 (attributed to the $^{239}Pu^{+}$ ions) and 255 (^{239}PuO) showed counts above background, mostly on the edges of the grain. The 239 image seemed to be correlated with Fe, and to a lesser extent to Al and Ca. In contrast to what we expected however, the 239 counts were in most cases higher than the 255 counts. The 239/255 ratio for this series of measurements varied between 0.7 and 4.1.

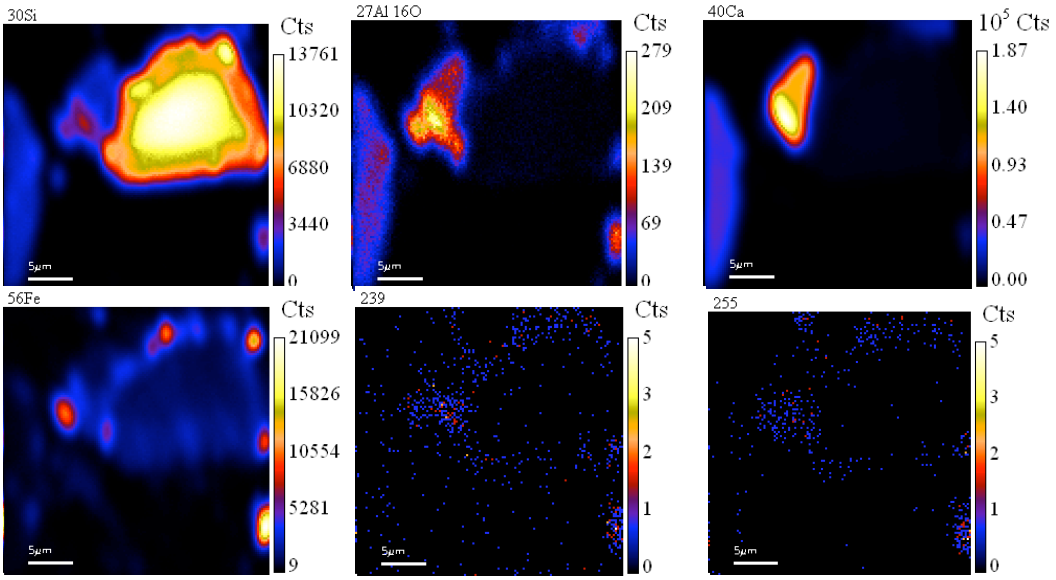

Figure C1. 30 x 30 µm ion images of ^{30}Si, ^{27}AlO, ^{40}Ca, ^{56}Fe, 239 (attributed to ^{239}Pu) and 255 (attributed to $^{239}Pu^{16}O$) showing increased secondary ion counts for 239 and 255 near the grain boundaries.

Invited Talk: Asian Pacific Symposium on Radiochemistry Nov. 29-Dec. 4, Napa CA, 2009

STRUCTURE OF PLUTONIUM COLLOID WHEN ASSOCIATED WITH DIFFERENT MINERALS

B.A. Powell, Z. Dai*, M. Zavarin*, A.B. Kersting*,

Clemson University, Dept. of Environmental Engineering and Earth Sciences, Clemson, SC 29625 USA
*Glenn T. Seaborg Institute, Physical & Life Sciences Directorate, Lawrence Livermore National Laboratory, 7000 East Ave., Livermore, CA 94550 USA,

Recent field studies have shown subsurface transport of Pu over Km length scales, where the Pu is associated with colloidal particles and not the dissolved fraction (e.g. [1], [2]). Yet despite these observations and a body of experimental and modeling studies, a comprehensive understanding of the mechanism of colloid-facilitated transport of Pu remains elusive. For example, very little is known about the geochemical and biochemical mechanisms controlling Pu-colloid formation and association. This lack of understanding limits our ability to model and predict transport.

In this study, we evaluated the surface structure of Pu with several minerals. Pu colloids were formed in oversaturated conditions ([Pu(IV)] = 10^{-6}M). Pu colloids were then sorbed to several minerals and its structure examined. Results using High-Resolution Transmission Electron Microscopy (TEM) show that when Pu colloids were formed in solution the expected fcc fluorite-type structure of PuO_2 was observed. When the Pu colloids were sorbed on the surface of silica the fcc fluorite-type structure of PuO_2 was also observed. However, when Pu colloids were sorbed to goethite {100} surfaces, the Pu colloid structure matched bcc Pu_4O_7 rather than fcc PuO_2. This structural distortion appears to be related to the lattice match that results in a strong parallel correlation between the goethite {021} crystal planes and the Pu_4O_7 {114} crystal planes. We speculate that the structural distortion of the Pu colloids results from a stronger interaction between Pu colloids and goethite surfaces, relative to silica surfaces and that this structural distortion will affect the solubility of Pu colloids.

[1] Kersting et al., *Nature.* **1999**, *397*, 56-59.
[2] Novikov et al., *Science.* **2006**, *314*, 638-641.

Funded by Office of Science, Biological & Environmental Research. Prepared by LLNL under Contract DE-AC52-07NA27344

Task D1: Molecular Scale Simulations

Methods for benchmarking ab initio electronic structure methods for the accurate description of aqueous Pu(IV) complexes

In our computational benchmark studies this year, the core electrons of Pu were replaced with the scalar relativistic effective core potential (ECP) of Hay and Martin, along with the associated basis set. A number of pseudo-potentials are available for actinides, including the energy-adjusted pseudopotentials of Dolg and co-workers, and the *ab initio* model potential (AIMP) of Seijo and co-workers. We choose the Hay and Martin ECP for its simplicity, as this is a benchmark study where we are mainly comparing differences across varying levels of theory and any systematic errors due to the choice of ECPs should not impact our conclusions. The Pu 6*s*, 6*p*, and 5*f* electrons are treated as valence. The ECP replaces the 78 core electrons, leaving 12 valence electrons for Pu(IV). Hay and Martin used a [3*s*3*p*2*d*2*f*] contraction; here, we decontract the two outermost *s* and *p* primitives to yield a [4*s*4*p*2*d*2*f*] contraction. Double-zeta correlation consistent basis sets (cc-pVDZ) are used for all electrons of O and H. The O atoms in OH^- are augmented with diffuse functions (aug-cc-pVDZ) in order to give a good description of the excess negative charge on the O.

Although spin-orbit effects can have a significant effect on the excited state spectrum, here we are primarily interested in ground state properties. In this case, a number of studies on small actinide complexes have demonstrated that spin-orbit effects on ground state properties are minor, thus this is neglected in our work here.

The complete active space self-consistent field (CASSCF) method is the most straightforward approach to account for the multi-configurational character of the *f*-electrons. The active space consists of four Pu *f*-electrons distributed over seven *f*-orbitals, i.e, a CAS(4/7) calculation. The optimized CASSCF wave function is then used as the reference for second-order, multi-reference Moller-Plesset (MRMP) perturbation theory, which is suitable for capturing dynamical correlation effects beyond CASSCF. In the MRMP calculations, the oxygen 1*s* electrons are taken as core while the remaining electrons are correlated. The MRMP is the highest level of theory we employ here and thus serves as the benchmark standard against which more approximate approaches are compared.

For comparison, we also consider standard MP2 theory from a single-reference, restricted open-shell Hartree-Fock (ROHF) reference function, using the reference determinant from the CASSCF wave function with the dominant weight.

Schemes such as DFT+U, where an additional Hubbard-like U-term is introduced to correct for *f*-electron self-interaction, can potentially mitigate the problem with standard DFT. Currently, efforts to use the DFT+U method is more appealing in that it does not incur as much computational effort beyond DFT, and can be readily employed in dynamical simulations. Current work is in progress to estimate U from first principles for use in a DFT+U model for aqueous Pu(IV). This work will continue in FY11

Computational studies would greatly benefit from a comparison with direct spectroscopic evidence such as EXAFS

Selection of resins for Pu(IV)-hydroxide XAS measurements:

Computational studies within this task have indicated that $Pu(OH)_4(aq)$ is stabilized as a planar structure in the presence of water. This is an unexpected distortion from the tetragonal structure The computational studies would greatly benefit from a comparison with direct spectroscopic evidence. However, this is complicated due to the low solubility of Pu hydrolysis products and high detection limits of applicable spectroscopies (e.g. EXAFS). In order to obtain meaningful spectroscopic data to examine the structure of aqueous Pu hydrolysis species, aqueous concentrations high enough for detection are required. To maintain high aqueous concentrations and limit precipitation of Pu hydrolysis products, ion exchange resins will be used to hold Pu(IV) as monomeric species. Commercial Eichrom and Dowex cation exchange resins were screened using Th(IV) as an analog for Pu(IV). These studies showed that Th(IV) is retained to 50 ppm and higher on the resins up to pH 5, where the $Pu(OH)_3^+$ and $Pu(OH)_4^o$ species will dominate. Therefore, XAS data may be obtained for monomeric Pu(IV) species associated with the ion exchange resins and yield useful information about the dissolved species.

Abstract Invited: ACS San Francisco, March 2010

Symposium Title: (GEOC004) Predicting Molecular Properties of the Mineral-Water Interface: Challenges and Opportunities for High Performance Computing

P. Huang and E. Schwegler. Structure and dynamics of liquid water on surfaces from ab initio molecular dynamics: Graphene/water and alumina/water

The behavior of solid/water interfaces at atomic scales is complex, and simulations can potentially provide useful insights. However, most simulations to date rely on simple, empirical models for interatomic interactions. The parameterization of such models is ambiguous; often they are fitted to bulk properties, and transferability to complex interfacial systems is uncertain. Instead, we report ab initio molecular dynamics simulations of solid/water interfaces, where interatomic interactions are derived on-the-fly from density functional theory. Two prototype examples are considered: graphene/water as a model hydrophobic surface, and alumina/water as a model oxide surface. In both cases, a bulk-like liquid water layer at ambient conditions is explicitly included. We examine interfacial structure and dynamics, and relate these to spectroscopic observables (infrared spectroscopy, nuclear magnetic resonance). Comparison to predictions from common empirical potentials is given in order to gain insight into when such models fail, and how they can be improved.

Abstract, Goldschmidt, June 13-18, Knoxville TN, 2010

Paramagnetic adsorption on silica as an analogue for actinide adsorption: A solid-state NMR study

HARRIS E. MASON, ROBERT S. MAXWELL AND SUSAN A. CARROLL7000 East Ave. Livermore, CA 94550 (mason42@llnl.gov, maxwell7@llnl.gov, carroll6@llnl.gov)

Many previous studies on actinide sorption have been preformed at high loading levels to maximize the possibility of observing the behavior with available instrumentation. However, some contaminated sites contain concentrations of actinides such as Pu from 10-8 M and lower, and it is unclear if high loading level experimental results are applicable. Therefore, the development of methods to measure relevant reactions at very low loadings is necessary. Here we developed solid sate nuclear magnetic resonance (NMR) techniques for analyses of actinide adsorption at low loadings.

The majority of actinides and actinide complexes exhibit paramagnetic electronic structures. The presences of even low amounts of paramagnetic cations can significantly affect the signal observed for other elements such as 1H or 29Si. These effects include, but are not limited to broadening, shifting, and relaxing the NMR signal. Quantification of these effects can allow indirect observation of actinide sorption.

We investigated the adsorption of paramagnetic cations such as Fe3+, Mn2+, and Ni2+ on silica surfaces at a range of low loading levels. The goals of this study were to develop these systems as 'safe' analogues to actinide systems where radiation and acute toxicity are a concern, and to determine the lowest loading level where paramagnetic effects on the NMR signal can be observed.

The loading level limits at pH = 6 were investigated by varying the paramagnetic cation concentration (<10 μM) and the silica substrate surface area (300 m2/g to ~4 cm2/g). We measured differences in the 1H spin-lattice, spin-spin, and rotating frame spin-lattice relaxation rates (1/T1, 1/T2, and 1/T1ρ respectively) for paramagnetic cations adsobed to silica. Given that 1H is the most abundant and sensitive nuclei in these systems, these rates should be influenced greatest by the presence of paramagnetic cations. Measuring differences in 1H T1ρ by 29Si{1H} cross-polarization magic angle spinning (CP/MAS) NMR can identify specific surface species which associate with paramagnets the strongest. Preliminary results from 29Si{1H} CP/MAS indicate that for mesoporous silica, Fe3+ absorbs preferentially to Q3 polymerized surface silanols over Q2 and Q4 sites.

Task E1: Survey of Pu-Interactive Microorganisms

Abstract submitted to the American Geophysical Union Fall Meeting, Dec. 15-19, 2010

Microbially Produced Organic Matter and Its Role in Facilitating Pu Transport in the Deep Vadose Zone

Jenny C. Fisher[1], Ruth M. Tinnacher[2], Mavrik Zavarin [2], Annie B. Kersting[2], Ken Czerwinski[3], and Duane P. Moser[1]

[1] Desert Research Institute, Division of Earth and Ecosystem Sciences, 755 E. Flamingo Rd., Las Vegas, NV 89119
[2] Glenn T. Seaborg Institute, Physical and Life Sciences Directorate, Lawrence Livermore National Laboratory, PO Box 808, Livermore, CA 94550
[3] Radiochemistry Program, Department of Chemistry- Radiochemistry, University of Nevada Las Vegas, 4505 Maryland Parkway, Box 454003, Las Vegas, NV 89154-4003

Microorganisms have the potential to affect the fate and mobility of actinides in the deep vadose zone (DVZ) by metabolism (direct oxidation/reduction and changes to ecosystem redox potential), production of colloids and ligands, or by sorption (biofilms). The role of microbial communities in colloid-facilitated Pu transport is currently under investigation at the Nevada Test Site (NTS). Our experimental objective is to obtain both qualitative and quantitative data on the *in situ* role of biological organic material (DOM, POC, and EPS) on the (de)sorption of Pu at environmentally relevant concentrations.

Groundwater samples were collected through vertical ventilation holes from a flooded post-test tunnel at the (NTS), where SSU rRNA gene libraries revealed a range of potential microbial physiotypes (J.C. Bruckner, unpublished data). Microbial enrichments were set up with the aim of isolating numerically significant representatives of major relevant physiotypes (e.g. aerobic heterotrophs, Mn/Fe reducers, EPS producers). NTS isolates and a well-characterized *Shewanella* (str. CN-32) were screened for their reactivity with Pu(IV). Organisms with both high and low (relative) K_d's were used in sorption and cell lysis experiments.

Viability experiments were conducted for all isolates in NaCl or NaCl/NaHCO3 solutions (I=0.01) for pH = 3, 5, 7, and 9. Products from cell lysis were filtered (0.22 µm) or dialyzed (MW cutoff = 20,000 kD). These fractions were normalized by TOC and equilibrated with Pu to determine if Pu sorbs more strongly to either viable cells, EPS, cell membranes, or cell exudates. In our experiments, Pu(IV) sorbed most strongly to cells with EPS (expolysaccharide, the major biofilm component). Results varied only slightly with different bacterial species. This suggests that changes in environmental conditions (e.g. pH, ionic strength) may lead to changes in Pu sorption on a biological basis as well as due to the known chemical effects. Thus the effects of microbial products should be considered when analyzing the potential for Pu mobility.